Physics – Uspekhi **45** (1) 27 – 57 (2002)

REVIEWS OF TOPICAL PROBLEMS PACS numbers: **05.45. – a**, **92.10. – c**, 92.20.Rb

Spatio-temporal pattern formation, fractals, and chaos in conceptual ecological models as applied to coupled plankton-fish dynamics

A B Medvinskiĭ, S V Petrovskiĭ, I A Tikhonova, D A Tikhonov,
B-L Li, E Venturino, H Malchow, G R Ivanitskiĭ

DOI: 10.1070/PU2002v045n01ABEH000980

Contents

Abstract. The current turn-of-the-century period witnesses the intensive use of the bioproducts of the World Ocean while at the same time calling for precautions to preserve its ecological stability. This requires that biophysical processes in aquatic systems be comprehensively explored and new methods for monitoring their dynamics be developed. While aquatic and terrestrial ecosystems have much in common in terms of their mathematical description, there are essential differences between them. For example, the mobility of oceanic plankton is mainly controlled by diffusion processes, whereas terrestrial organisms naturally enough obey totally different laws. This paper is focused on the processes underlying the dynamics of spatially inhomogeneous plankton communities. We demonstrate that conceptual reaction-diffusion mathematical models are an appropriate tool for investigating both complex spatio-temporal plankton dynamics and the fractal properties of planktivorous fish school walks.

A B Medvinskiĭ, I A Tikhonova, D A Tikhonov, G R Ivanitskiĭ
Institute for Theoretical & Experimental Biophysics,
Russian Academy of Sciences,
142290 Pushchino, Moscow Region, Russian Federation
Tel. (7-095) 923 96 68; (7-095) 923 74 67 (ext. 243)
Fax (7-0967) 79 05 53
E-mail: medvinsky@venus.iteb.serpukhov.su
S V Petrovskiĭ P P Shirshov Institute for Oceanology,
Russian Academy of Sciences,
Nakhimovskiĭ prosp. 36, 117218 Moscow, Russian Federation
B-L Li Department of Biology, University of New Mexico,
Albuquerque, NM 87131-1091, USA
E Venturino Dipartimento di Matematica, Politecnico di Torino,
corso Duca degli Abruzzi 24, 10129 Torino, Italy
H Malchow Institute for Environmental Systems Research,
Osnabrueck University, Artilleriestr. 34, Osnabrueck, 49069 Germany

Received 26 March 2001, revised 23 April 2001
Uspekhi Fizicheskikh Nauk **172** (1) 31 – 66 (2002)
Translated by Yu V Morozov; edited by M S Aksent'eva

"Nature's health was undermined by man. Man was unable to visualize Earth as a suffering living creature".
D Granin *Zubr* (Auroch)

1. Introduction

1.1 Why did Babylon fall?

Local catastrophes resulting from human interference in nature are nothing very new. Of late, however, all layers of society appear to be concerned about the threatening situation which is increasingly featured in the press.

On the one hand, the proliferation of industrial activities brings with it acid rains killing vegetation and discharge of harmful residues into the air which are responsible for the rapid enlargement of ozone holes and the associated increase of solar radiation exposure that may cause a rise in the frequency of genetic and oncologic diseases. The extensive use of chemical fertilizers and pesticides in agriculture has resulted in food quality degradation and river water pollution threatening the depletion of the available drinking water resources. Air pollution is a principal cause of the upward trend in bronchitis, asthma, and other diseases. The Chernobyl accident gave rise to concern about the safety of nuclear power production. Examples of upset ecological balance that

cloud the life of modern man are numerous, and rapid economic developments have a boomerang effect on human health.

On the other hand, the world population has recently turned six billion. Over the last quarter of the 20th century, 3,000 cities developed into urban agglomerations, with 1 million inhabitants each, to accommodate the growing population. The progress in science brought an improvement in the overall life expectancy. Campaigns against infectious diseases reduced their influence; developments in medicine and technology forced specialists to revise the concepts of birth and death. In the past, man's viability was the sole subject open for discussion in this context. Today, whether man is doomed to die or not has come to be seriously considered.

Such is reality. How can we reconcile the need for further economic growth and the conservation of nature as the human environment? Where is the way out of this conflicting situation? Does not mankind find itself in a trap from which it is impossible to escape except at the expense of great losses? Are we not close to the 'X-hour' when the planet's ecosystem must collapse under the tremendous human pressure?

Let us turn to an example from the remote past. The historian and geographer L N Gumilev relates in his book *Etnogenez i Biosfera Zemli* (Ethnogenesis and the Earth's Biosphere) why only ruins remain where Babylon (Babylonian Bab-Ilu, 'Gates of the God') stood at the height of its splendour in former times. It should be mentioned at the very beginning that Gumilev's hypothesis finds both advocates and opponents amongst specialists.

Despite a few lapses noticed by historians, the book by L N Gumilev is not devoid of interest [1]. Specialists studying the complex behaviour of spatially extended nonlinear systems easily perceive the author's stream of thought concerning the relationship between man and nature: on the one hand, nature can directly or indirectly influence social processes; on the other hand, there is an ever-increasing human impact on the environment.

Here is how L N Gumilev describes the fall of Babylon. The economy of Babylonia, an ancient state in southern Mesopotamia (now in Iraq), was based on irrigated agriculture using water of the Tigris and Euphrates for the purpose. The flow of water in irrigation canals was fast enough to avoid salinization of fertile soil and deposition of sand and gravel brought in from the Armenian Highland.

In 582 BC, Nebuchadnezzar II (Nebuchadrezzar or Nabuchodonosor), the ruler of Babylon, married princess Nitocris to strengthen the peace with Egypt. The princess was accompanied to Babylon by a suite of Egyptian advisers. Nitocris (presumably counselled by her advisers) proposed to dig a new canal to enlarge the irrigated area. The king approved the project, and the Pallukat (Pallakopas) canal was built during the 560s BC. It ran from the Euphrates upstream of Babylon and ensured irrigation of vast lands outside the floodplain, bringing great economic benefits. But the project had lasting repercussions. Opinions differ, however, among specialists as to whether the canal prolonged the existence of Babylon or precipitated its decline (as L N Gumilev and some others believed it did).

The river stream slowed down because a large fraction of its water went into the new canal. Particulate matter deposited by the water flow choked canals. The irrigation network became more and more expensive to maintain. The Pallukat water running across arid lands caused widespread soil salinization. Irrigated agriculture soon became costly and unprofitable. In 324 BC, Babylon still remained a large picturesque city, and Alexander the Great planned to make it the capital of his empire. However, the results of faulty irrigation practices became irreversible, the population declined, and by the beginning of the Christian era Babylon lay in ruins. The formerly splendid city with almost 1 million inhabitants was first reduced to a small settlement and then disappeared. Only a legend remembers the rich and powerful Babylonia.

That soil salinization was the only (or main) cause of Babylon's decline might be objected to as an overstatement. It can not be excluded, however, that the construction of the new canal was a gross mistake that undermined Babylon's economy and made it vulnerable to attack by numerous enemies. The ecological crisis in Mesopotamia lasted a few centuries. It formed the background against which faster social processes developed, certainly in close relation to environmental changes [2].

The history of the fall of Babylon is a parable for its descendants. Times change, and the cost of errors rises while the term of payment shortens. The present paper is concerned with the important question of how to organize environmental monitoring and ensure prediction of an oncoming disaster. Soil science has already developed a variety of tests for the evaluation of the condition of terrestrial ecosystems. Similar methods for the characteristic of processes in the world's ocean remain to be elaborated. Because experiments in nature may have dangerous consequences, such diagnostic systems should be based on mathematical models adequately describing the spatio-temporal dynamics of the environment on different spatial and temporal scales. In this context, the dynamics of the world's ocean and its ecosystems need to be described in terms of new notions (chaos, bifurcation, fractals, catastrophes) ensuing from the general laws of the theory of nonlinear nonequilibrium systems and specific functions of aqueous biological communities.

1.2 Patterns in nonlinear nonequilibrium systems

The problem of elucidation of pattern formation mechanisms in complex nonlinear systems is a central one in natural sciences, humanities, and technology [1 – 3]. The discovery of multiple steady states and transitions from one state to another as a result of critical fluctuations, excitability, oscillations, waves, and, in the general case, emergence of macroscopic order from microscopic interactions in various nonlinear nonequilibrium natural and social systems has given an incentive to many theoretical and experimental studies aimed at investigating these phenomena.

The classical approach to identifying the origin of spatial structures was pioneered by Turing [4] and further developed by his followers (references to some of their works can be found in Ref. [5]). The results of these studies indicate that an initially uniform distribution of reacting components may lack stability. As the instability increases, a spatially nonuni-

[1] English translation of the book see on the website http://www.cossackweb.com/gumilev/ — *Editor's note*.

[2] The reader can find an extension of this instructive story about the interplay between man and nature in the territory of ancient Iraq in a paper by A Yu Morst entitled "Ancient and present-day desertification in Iraq" and published in the journal *Problemy Osvoeniya Pustyn'* (Problems of Desert Development), No. 2, 1984. — *Author's note*.

form distribution (spatial pattern) of reaction activators and inhibitors occurs. Turing pattern formation is based on the coupling of linear diffusion and local nonlinear kinetics of the reaction under conditions in which the diffusivity of the activator is lower than that of the inhibitor. Recent experimental studies reported by De Kepper and co-workers [6] have demonstrated the formation of Turing structures in the context of chemical interactions [3].

A major unresolved problem in the framework of the Turing approach is that there is still no clear identification of activators and inhibitors which could be involved in the formation of patterns of different nature (physico-chemical, biological or social); moreover, such an identification seems hardly possible at all. Today, more realistic approaches are being developed to address the pattern formation theory. With these approaches, the complex spatio-temporal dynamics of open spatially confined systems is considered to be a result of the interplay between their intrinsic dynamics and external impacts coming from the environment. In ecology, such interactions may involve both physico-chemical and biological factors. The present paper is focused on biological factors influencing the dynamics of aquatic communities. It examines the role of predator invasion, planktivorous fish cruising, and the interlinks of neighbouring habitats in the formation of complex and variable spatio-temporal plankton patterns widespread in the ocean.

1.3 Plankton and plankton dynamics models

Plankton are floating organisms of many different phyla inhabiting the upper layers of the open ocean, freshwater bodies, and greater rivers. The distribution of these organisms is to a large extent dependent on water movements [9–11]. Their functional classification is based on the size, trophic level, and distribution patterns in natural waters. Autotrophs or primary producers make up phytoplankton while heterotrophs, i.e. consumers, comprise both bacterioplankters and zooplankters. Classification in terms of size is possible because planktonic organisms are differentially retained by the aperture of plankton nets and filters. *Picoplankton*, which consists of forms less than 2 μm in size, is distinguished from *nanoplankton* (0.2–2 mm), *macroplankton* (2–20 mm), and *megaplankton* (over 20 mm) [11, 12].

Antoine van Leeuwenhoek, the founder of microscopy, was probably the first man to observe, as long ago as the 17th century, minute creatures, which he called *animacules*, in a drop of pond water [13]. The German scientist Victor Hensen, an organizer of the first big German oceanographic expedition of 1889 [14, 15], coined the term *plankton* [from the Greek *planktos*, meaning 'made to wander (or to drift)'].

Phytoplankton are microscopic plants on which the life and development of practically all marine communities are dependent. Because phytoplankton carries out photosynthesis, the world stock produces half of the total oxygen needed to maintain the existence of mankind and consumes half of the carbon dioxide that might otherwise contribute to global warming. Phytoplankton recycles other particulate and gaseous substances, besides oxygen and carbon, such as phosphorous, nitrous, and sulphur-containing compounds [16–18]. Therefore, phytoplankton may be regarded as a main factor involved in the control of the further development of the Earth's climate, and there is voluminous literature in support of this view (see, for instance, Refs [19, 20]).

Zooplankton are planktonic animals. Marine zooplankton comprise both phytophagous and predatory organisms. The former graze on phytoplankton and are preyed upon by carnivorous zooplankters. Collectively, phytoplankton and zooplankton form the basis of all oceanic food chains and webs. In its turn, the reproduction of plankton-forming species depends on many environmental factors, such as water temperature and salinity, solar radiation, nutrient availability, etc. [9, 12]. The temporal variability of plankton species composition is caused by seasonal changes and (in accord with a concept originating from the works of Lotka [21] and Volterra [22]) 'predator–prey' trophic relationships between zooplankton and phytoplankton.

Because of its obvious importance, the dynamics of planktonic systems has been continuously investigated for over 100 years. It is worthwhile to note that practically from the very beginning regular plankton studies have combined field observations, laboratory experiments, and the construction of mathematical models. In the 19th century, an interest in plankton dynamics was greatly stimulated by fishery which then discovered a strong positive correlation between the abundance of fish and zooplankton. The aforementioned German plankton expedition of 1889 was initiated by fishing enterprises. At about the same time, an incentive was given to the development of scientifically-based commercial fishing. In the early 20th century, the first mathematical models were designed to better understand and learn to predict fish stock dynamics and its correlations with biological and physical factors taking into consideration the human impact on the environment (see, for instance, Refs [23–25]).

The foundation of modern mathematical simulation of the processes underlying phytoplankton production was laid by the works reported in Refs [26–29] and some others. These studies were reviewed by Droop [30]. A collection of the most popular models has been recently depicted by Behrenfeld and Falkowski [31].

Fleming [26] was the first to use ordinary differential equations describing phytoplankton biomass dynamics for the simulation of control of sharp rises in phytoplankton density (water blooms) by zooplankton. Other approaches included the construction of functions based on observations of natural phenomena [32] and the application of the classical Lotka–Volterra equations to the description of predator–prey relationships between zooplankton and phytoplankton [33–36]. A more realistic description of zooplankton grazing and its functional dependence on phytoplankton abundance was proposed by Ivlev [27]. This approach with slight modifications was later employed by Mayzaud and Poulet [37]. In addition, functional plankton reactions are frequently described by widely-used mathematical expressions from the Monod and Michaelis–Menten [38–40] saturation models which provide the basis for all kinetic studies of enzymes (see, for instance, Refs [41–48]). The observed temporal patterns boil down to stable oscillations well-known to occur in predator–prey systems and also to oscillatory or monotonic relaxation to one of the many conceivable steady states. In connection with this, excitable systems are of special interest because their characteristically long times of relaxation toward a steady state following a supracritical external perturbation, such as a sudden rise of temperature or nutrient inflow, fit them for the simulation of the so-called *red* or *brown tides* [47–50].

[3] A discussion of the results pertaining to other types of spatial patterns is beyond the scope of this communication; see, for example, Refs [7, 8]. — *Author's note*.

Of special interest in the context of time-related changes in plankton species composition are limitations on their predictability. In the early studies, mathematical models of marine ecosystems were developed based on the belief that the predictive value of a model increases with increasing number of explicitly included species. As a result, many multi-species models were proposed which took into consideration the detailed food web structure in a given community (see, for example, Refs [51 – 53]). However, the real predictive value of such models is not very high and seldom exceeds a few weeks. Indeed, the more variables a model includes the lower its predictive value. This obvious paradox can be explained in terms of dynamic chaos [54]. In connection with this, it should be noted that notwithstanding the absence of a strict proof of chaotic behaviour in natural populations, there is an increasingly large amount of definitive evidence in favour of it [45, 55 – 57]. The hypothesis of chaotic population dynamics introduces quite a different view of system predictability (see, for example, Ref. [55]) and makes conceptual models, i.e. models considering interactions between few species, as useful as many-species ones. Moreover, *few-species models are sometimes even more helpful because they take into account only basic specific features characterizing functional patterns of a given community* (see, for instance, Refs [58 – 60]).

The dynamics of systems perturbed from the outside is another interesting problem. Such ideal periodic perturbation arises naturally, being related to circadian, seasonal, and annual cycles of solar radiation determining the rate of photosynthesis, water temperature, food availability, and other factors [61 – 64]. Certainly, some external noise is superposed on these perturbations under natural conditions. Thus far, few models of complete food chains or their fragments have been examined starting with nutrient matter, phytoplankton and zooplankton and ending with planktivorous fish; a variety of transition routes to chaotic dynamics have been identified [45, 65 – 72].

Plankton density is time-related and depends on spatial coordinates. Numerous field studies have demonstrated the clear-cut spatial heterogeneity of plankton distribution known as 'patchiness' [73 – 75]. This phenomenon is apparent on all spatial scales from centimeters to kilometers. Various hypotheses have been suggested to account for the patchiness of plankton distribution. Specifically, seawater turbulence [78] and nonuniform temperature fields [79] in the ocean were considered as factors responsible for the formation of such plankton patterns. The appearance of well-known linear plankton structures was attributed to trapping floating microorganisms in Langmuir circulation cells [80, 81]. Other physical mechanisms underlying steep density gradients of plankton distribution were postulated, e.g. upwelling of nutrient-rich waters [223], local temperature differences, turbulent mixing, and internal waves [82 – 84].

Moreover, on small spatial scales (tens of centimeters) and under relatively uniform physical conditions, the difference between 'diffusive' mobility of individual organisms and their locomotory ability may result in even smaller spatial aggregations, e.g. under the effect of bioconvection and gyrotaxis [85 – 88]. Thus far, a mechanism of diffusion-limited spatial aggregation [89] has been proposed and experimentally verified for certain bacteria, if not for plankton, known to form the so-called fingering colonies [90, 91].

In other words, mathematical models of plankton population dynamics must take into account not only the growth rate and interactions but also spatial processes, such as random or directed, concerted or relative motions of different species, as well as environmental changes. It is widely accepted that interactions between phytoplankters and zooplankters coupled to their transport are responsible for the known diversity of spatio-temporal planktonic structures (including *patchiness*; see, for instance, Refs [73, 92]). 'Reaction – diffusion' and probably advection equations should be used for mathematical simulation of these phenomena. A good introductory review of relevant studies was published by Holmes et al. [93].

Since the classical work by Turing [4] on the role of nonequilibrium reaction-diffusion patterns in morphogenesis, dissipative mechanisms of spontaneous formation of spatial and spatio-temporal structures in a uniform environment have remained in the spotlight of theoretical biology and ecology. Turing showed that a nonlinear interaction of at least two agents having significantly different diffusion coefficients may result in a spatial structure. Segel and Jackson [33] were the first to apply Turing's ideas to population dynamics in a study on dissipative instability of predator – prey relationships using interactions between algivorous crustaceans (showing a higher mobility than algae) and phytoplankton as a model. Levin and Segel [35] proposed this scenario of spatial structure formation as a possible source of plankton patchy distribution. Recent studies [46, 94] have demonstrated the possibility of realizing such regimes as local biostability, limit-cycle oscillations in a predator – prey system, plankton front propagation, formation and drift of Turing's plankton patches in the minimal model of phytoplankton and zooplankton interactions proposed by Scheffer [44] to elucidate effects of nutrients and planktivorous fish on alternative types of local equilibrium in plankton community dynamics.

Kierstead and Slobodkin [95] (see also Ref. [96]) appear to have been the first to pose the problem of critical size of plankton patches by presenting what is currently known as the KISS model which couples exponential growth to diffusion in an isolated population. In their model, patches are explicitly unstable because the relationship between exponential growth and diffusion leads to an explosive spatial spread of the initial patch of planktonic organisms. Surprisingly, the speed of the diffusion front turns out to be equal to the asymptotic speed of a logistically growing population [97 – 99].

Allee's populations [100, 101], in which the critical condition of the species is responsible for one of the two stable states leading either to extinction or survival at a given saturation capacity, also depend on a critical spatial size [102 – 107]. Spatially limited populations whose size exceeds the critical one survive while smaller ones die out. However, neither bistability nor critical spatial size is necessarily associated with Allee's effect. Indeed, two stable states and the related hysteresis loops can also arise in a predator – prey system where the prey propagation submits to the logistic law while the functional predator response to variations in the prey population density may be of type II or III (see, for instance, Refs [109, 110]).

Consideration of the dynamics of a predator – prey system reveals a wide range of spatial and spatio-temporal patterns, such as regular and irregular oscillations, propagating fronts, concentric and spiral waves, pulses, and stationary spatial structures. Many of these patterns first became known from the examination of oscillatory chemical reactions (see, for instance, Ref. [110]) but were never observed to occur in

natural plankton populations. However, spiral waves were seen in the ocean as rotary motions of plankton patches on a kilometer scale [111]. Furthermore, they were found to play an important role in parasitoid – prey systems [112]. As regards other motile microorganisms, stationary structures and travelling waves resembling targets or spirals were reported to occur in various bacterial colonies and slime mould (*Dictyostelium discoideum*) populations [113 – 135]. These cells are chemotactic strains capable of upward movement along the gradient of a chemical attractant. *Chemotaxis* is a form of density-dependent cross-diffusion. The interesting question of whether there is a prey taxis in plankton populations remains to be clarified.

It is important that consideration of spatial extension and function of a plankton community reveals new routes to chaotic dynamics. Pascual [58] described the appearance of diffusion-induced spatio-temporal chaos along a linear nutrient gradient. Chaotic oscillations behind propagating diffusion fronts were recorded in a predator – prey system (see, for instance, Refs [136, 137]); a similar phenomenon occurred in a mathematically similar model of a chemical reactor [138, 139]. Recent studies have demonstrated that chaotic spatio-temporal oscillations in predator – prey systems are in a sense a somewhat more general phenomenon not necessarily associated with front propagation or heterogeneity of environmental parameters [59, 60].

Malchow [141, 142] cited an example of structures arising in the Scheffer model. He also derived conditions for the emergence of three-dimensional spatial and spatio-temporal patterns in spatially homogeneous populations resulting from instabilities induced by a differential flow [140]. Instabilities in the spatially uniform distribution may arise if phytoplankton and zooplankton travel with different velocities regardless of which velocity is higher. This mechanism of generating patchy patterns is more general than the Turing mechanism which imposes strong limitations on the diffusion coefficient. Hence, a wide range of its potential applications to population dynamics.

It follows from the above that plankton community dynamics including pattern formation processes have been extensively investigated during the past decades. This greatly promoted the understanding of major distinctive functional features of plankton systems. For all that, many mechanisms of spatio-temporal variability of plankton populations await clarification. Biological processes are to a large extent dependent on such prominent physical patterns as thermoclines, upwelling, fronts, and vortices (see Section 4 for a more detailed discussion). However, temporal and spatio-temporal variability may result from the relationship between nonlinear biological processes and nonlinear physico-chemical dynamics even under relatively uniform physical conditions [35, 42, 43]. Daly and Smith [143] arrived at the conclusion "...that in structured biological communities, biological processes may be more important on smaller scales where the behaviour, such as vertical migration or predation, may control the plankton production whereas physical processes may be more important on larger scales ...". In order to be able to distinguish between parameter regions dominated by biological or physical processes, O'Brien and Wroblewski [144] introduced a dimensionless parameter containing the characteristic water speed and maximum species-specific biological growth rate (see also Refs [145, 146]).

Physical and biological processes may be significantly different not only on spatial but also on temporal scales. For example, the effects of external hydrodynamic factors on the formation and stability of nonequilibrium spatio-temporal plankton structures were demonstrated on a Scheffer model using the separation of different time scales of biological and physical processes [147]. A channel under the tidal force with relatively large biomass retention time served as the model hydrodynamic system. The following phenomena characterized by different time scales were considered: the simple physical transport and deformation of an initially nonuniform spatial plankton distribution and the formation of a localized spatial maximum of phytoplankton biomass determined by biological processes.

The formation of plankton patterns strongly depends on the interaction between various physical (light, temperature, hydrodynamics) and biological (nutrient supply, predation) factors (see, for instance, Refs [73, 78, 79]). Under natural conditions, the direction of plankton patch motion does not always coincide with the water flow direction [111, 148]. At characteristic spatial sizes in excess of about 100 m, the phytoplankton behaviour progressively deviates from that of simple passive matter dispersed by turbulence [149, 150]. Similarly, on scales of less than tens of kilometers, variability of zooplankton abundance in space is significantly different from spatial environmental variations [151]. This indicates that biological factors play an important role in the generation of plankton patchiness [41]. The question arises of whether biological factors, such as growth and interaction in a predator – prey system, can be responsible for plankton pattern formation in the absence of hydrodynamic effects.

The present paper presents conceptual models with a small number of trophic links in order to demonstrate that predator – prey interactions can give rise to complex spatio-temporal dynamics of both plankton and plankton-fish communities.

2. Complex patterns in a simple 'minimal' plankton dynamics model

2.1 Mathematical model

This section considers the spatio-temporal dynamics of an aquatic community in terms of a two-species predator – prey (i.e. zooplankton – phytoplankton) system. We demonstrate that such a simple model can adequately describe the formation of patchy spatial distribution of a species.

Based on a widely-accepted approach [152, 153], the functioning of a predator – prey community can be described by the following system of 'reaction – diffusion' equations:

$$\frac{\partial u}{\partial t} = D\,\Delta u + f(u,v)\,, \tag{2.1}$$

$$\frac{\partial v}{\partial t} = D\,\Delta v + g(u,v)\,. \tag{2.2}$$

Here, $u(\mathbf{r},t)$ and $v(\mathbf{r},t)$ denote the prey and predator density respectively, $\mathbf{r}$ is the position, t is time, D is the diffusion coefficient, and Δ is the Laplace operator. The two species are assumed to show equal diffusivity which is normally true of natural plankton communities where mixing is largely due to seawater turbulence. The form of the functions $f(u,v)$ and $g(u,v)$ is determined by local biological processes in a given community and, for biological reasons, can be described in

the following way:

$$f(u,v) = P(u) - E(u,v)\,,$$

$$g(u,v) = k^* E(u,v) - \mu v\,.$$

The function $P(u)$ describes the local growth and natural mortality of the prey whereas $E(u,v)$ stands for predation, i.e. trophic interaction between the prey and the predator. The term μ is the predator mortality rate, and the coefficient k^* describes effectiveness of food utilization.

The choice of functions $P(u)$ and $E(u,v)$ in Eqns (2.1), (2.2) may vary depending on the type of prey population and functional response of the predator to changes in prey density. It is assumed, based on the results of field and laboratory observations of plankton system functioning [12, 73], that the local growth of a prey population is logistic while the predator displays a Holling type II functional response. By choosing the simplest mathematical expressions for functions $P(u)$ and $E(u,v)$ [152], the following equations are obtained:

$$\frac{\partial u}{\partial t} = D\,\Delta u + \frac{\alpha}{b}\,u(b-u) - \gamma\,\frac{u}{u+H}\,v\,, \tag{2.3}$$

$$\frac{\partial v}{\partial t} = D\,\Delta v + k^*\gamma\,\frac{u}{u+H}\,v - \mu v\,, \tag{2.4}$$

where α, b, H, and γ are constants, with α standing for the maximum growth rate of the prey, b being the carrying capacity of the prey population, and H — the half-maximum prey population density. It should be noted that a more detailed parameterization is hardly sensible in such a schematic model describing interactions between a small number of species as the (2.1), (2.2) model. Assuming that

$$\widetilde{u} = \frac{u}{b}\,, \qquad \widetilde{v} = \frac{v\gamma}{\alpha b}\,, \qquad \widetilde{t} = \alpha t\,, \qquad \widetilde{\mathbf{r}} = \mathbf{r}\left(\frac{\alpha}{D}\right)^{1/2} \tag{2.5}$$

and introducing new dimensionless parameters $h = H/b$, $m = \mu/\alpha$, and $k = k^*\gamma/\alpha$, the following equations containing only dimensionless quantities are derived from (2.3), (2.4):

$$\frac{\partial u}{\partial t} = \Delta u + u(1-u) - \frac{u}{u+h}\,v\,, \tag{2.6}$$

$$\frac{\partial v}{\partial t} = \Delta v + k\,\frac{u}{u+h}\,v - mv \tag{2.7}$$

(here and hereinafter, tildes are omitted). Certain comments and a more detailed consideration of the choice of dimensionless variables for the (2.3), (2.4) system can be found in Ref. [60].

Before proceeding to the examination of spatio-temporal pattern formation, it appears appropriate to consider local system dynamics, i.e. properties of Eqns (2.6), (2.7) without diffusion terms. It is easy to show by the linear stability analysis that the system

$$\begin{aligned} \frac{\partial u}{\partial t} &= u(1-u) - \frac{u}{u+h}\,v\,, \\ \frac{\partial v}{\partial t} &= k\,\frac{u}{u+h}\,v - mv \end{aligned} \tag{2.8}$$

possesses three stationary states: $(0,0)$ or total extinction; $(1,0)$, i.e. extinction of the predator; (u_*, v_*), i.e. prey/predator coexistence, where

$$u_* = \frac{rh}{1-r}\,, \qquad v_* = (1-u_*)(h+u_*)\,, \tag{2.9}$$

$r = m/k$. It is easy to see that $(0,0)$ is a saddle-point for all non-negative values of k, m, and h. The stationary point $(1,0)$ is a saddle-point if the nontrivial point (u_*, v_*) lies in the biologically meaningful region $u > 0$, $v > 0$; otherwise, it represents a stable node. The stationary point (u_*, v_*) can be of any type.

It is worthwhile to note that the coexistence state (u_*, v_*) is shifted toward a biologically meaningful region $u > 0$, $v > 0$ when

$$h < \frac{1-r}{r}\,, \tag{2.10}$$

and becomes unstable at

$$h < \frac{1-r}{1+r}\,. \tag{2.11}$$

In the latter case, the steady state is surrounded by a stable limit cycle and the system is characterized by oscillatory kinetics.

These results provide useful information on the choice of parameters for the numerical integration of Eqns (2.6), (2.7). In the case of existence of a stable stationary point in the phase space of the system (i.e. when condition (2.10) is satisfied and condition (2.11) is broken), the system dynamics is usually reduced to the relaxation toward a stable spatially homogeneous state (u_*, v_*). Details of this process depend on the initial conditions; for example, in the case of a finite initial distribution of the species, the relaxation is normally achieved after the propagation of diffusion fronts [152, 154 – 156]. Further discussion will be mostly focused on the formation of short-living spatio-temporal patterns and the parameter region satisfying condition (2.11).

2.2 One-dimensional models

The spatio-temporal dynamics of 'reaction – diffusion' systems to a large extent depends on the choice of initial conditions. Specific features of the initial species distribution in natural communities can be attributed to concrete causes. The spatially homogeneous initial conditions represent the simplest form of the initial spatial distribution. In this case, however, the species distribution remains uniform at any time, and no spatial patterns can emerge. Nontrivial spatio-temporal dynamics can be obtained by the introduction of a perturbation into the initially uniform distribution.

In this section, we concentrate on the one-dimensional dynamics of the system (2.6), (2.7). A variety of disturbed initial conditions are considered. To begin with, there is a constant-gradient distribution

$$u(x,0) = u_*\,, \tag{2.12}$$

$$v(x,0) = \varphi_1(x) = v_* + \varepsilon x + \delta\,, \tag{2.13}$$

where ε and δ are certain parameters.

The results of computer simulation indicate that the type of system dynamics is determined by quantities ε and δ. In the case of a small ε, the initial conditions (2.12), (2.13) evolve into a smooth heterogeneous spatial distribution of the species [59]. Such spatial distributions tend to gradually vary

in time, and the local temporal behaviour of variables u and v follows the limit cycle of a homogeneous system. This regime is not self-contained, and the smooth spatial pattern arising in this case slowly relaxes to the spatially uniform species distribution [60].

However, for another set of parameters (e.g. when the gradient exceeds a certain critical value, $\varepsilon \geqslant \varepsilon_{\rm cr}$, where $\varepsilon_{\rm cr}$ depends on δ), the species spatial distribution is substantially different (cf. [59]). Figure 1 illustrates such a spatial distribution at the moments $t = 640$ (a) and $t = 2640$ (b) obtained at $k = 2$, $r = 0.4$, $h = 0.3$, $\varepsilon = 10^{-6}$, and $\delta = -1.5 \times 10^{-3}$. In this case, the initial distribution (2.12), (2.13) results in the appearance of strongly irregular sharp transient patterns inside a sub-domain of the system (Fig. 1a). The area occupied by such a structure increases with time, and the irregular spatio-temporal oscillations eventually prevail throughout the entire domain (Fig. 1b). Importantly, this regime is a persistent one. Long-time numerical simulations show that the system dynamics undergoes no further changes after irregular spatio-temporal oscillations spread over the entire domain.

In this case, the temporal behaviour of concentrations u and v also becomes completely different. Figure 2a shows a 'local' phase plane of the system obtained at a fixed point

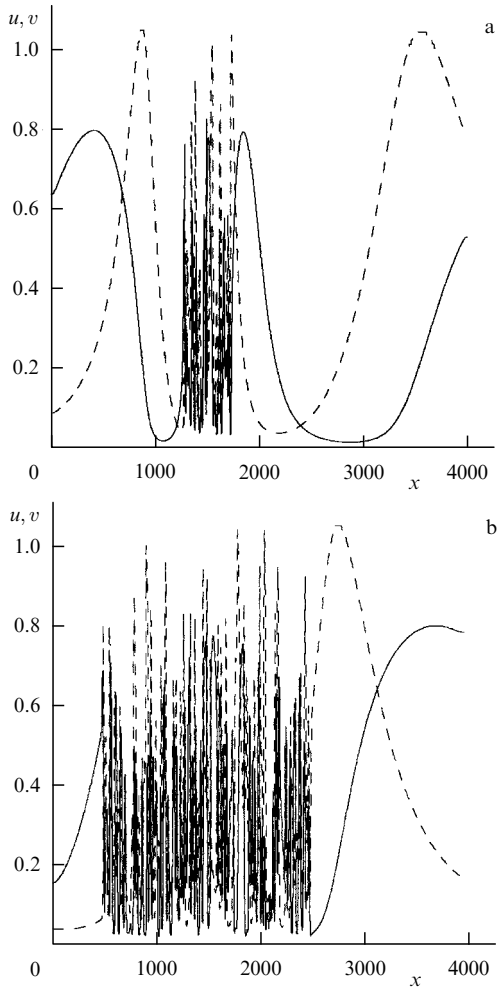

Figure 1. Spatial distribution of populations (solid line — prey, dashed line — predator) calculated for a case where the 'regular phase' is gradually displaced leading to the onset of a 'chaotic phase'; (a) $t = 640$, (b) $t = 2640$.

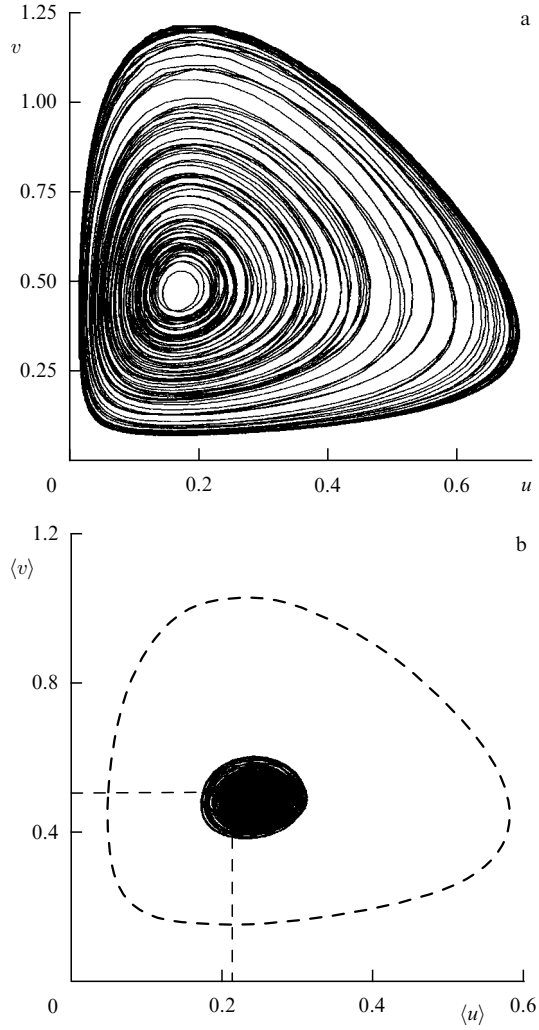

Figure 2. Phase planes of a system obtained at a fixed point inside the domain occupied by irregular spatio-temporal oscillations (a) and changes of spatially averaged prey and predator densities calculated for a case of irregular system dynamics (b); parameters are given in the text. The dashed line (b) shows the limit cycle of a spatially homogeneous system; the straight lines indicate the position of the steady state.

$\bar{x} = 480$ inside the region invaded by irregular spatio-temporal oscillations. Now, the trajectories fill almost the entire domain within the limit cycle (such a cycle characterizes smooth pattern formation). It will be shown below that this dynamic regime of the system corresponds to spatio-temporal chaos (see Ref. [59]).

A remarkable property of such system dynamics is the spread of the irregular pattern over the entire domain so that, at any moment, there are boundaries separating regions with different dynamic regimes, i.e. regions where sharp irregular patterns arise and those with smooth regular patterns. The results of our numerical experiments indicate that these interfaces propagate in opposite directions at an approximately constant speed; as a result, the chaotic dynamics region always increases. This phenomenon is an essentially spatio-temporal one, that is *chaos exists because the chaotic regime 'displaces' the regular one*. Such dynamics of the system appears to resemble the transition between regular and chaotic 'phases'.

Because the spatial distribution of species abundance is essentially non-uniform, the most informative approach

appears to be such that considers specially introduced quantities taking into account both temporal dynamics and spatial extension of the system. The spatially averaged density of organisms provides the simplest example of such quantities (other examples will be given below). Figure 2b presents dynamic changes in a phase space $(\langle u\rangle, \langle v\rangle)$ at the following values of parameters:

$$k = 2.0\,, \qquad r = 0.33\,, \qquad h = 0.43\,.$$

As the trajectory corresponding to the smooth pattern (not shown in the figure) slowly approaches the limit cycle (dashed curve), that corresponding to the regime in which a clear-cut spatial pattern arises remains in close proximity to the steady state $\langle u\rangle = u_*$, $\langle v\rangle = v_*$ and fills the space within a certain domain with a diameter significantly smaller than the limit cycle diameter. This means that the amplitude of time-related changes of the spatially averaged species abundance is much smaller in the case of smooth regular patterns.

It is worth noting that the 'two-phase' dynamics of system (2.6), (2.7) described above can not be attributed to a selective choice of initial conditions in the form (2.12), (2.13). Specifically, for the initial conditions

$$u(x,0) = u_*\,, \tag{2.14}$$

$$v(x,0) = v_* \quad \text{for} \quad x \leqslant x_0 \quad \text{or} \quad x \geqslant x_0 + S\,, \tag{2.15}$$

$$v(x,0) = v_* + A\sin\left(\frac{2\pi(x-x_0)}{S}\right) \quad \text{for} \quad x_0 \leqslant x \leqslant x_0 + S$$

the spatially uniform distribution (with periodic changes in time characteristic of the limit cycle) 'survives' only at very low values of amplitude A and/or perturbation S (see Ref. [60] for a detailed analysis). For somewhat higher (yet rather small) A and S, the initial distribution (2.14), (2.15) evolves into clear-cut irregular spatio-temporal patterns. The 'embryo of the chaotic phase' first appears in the vicinity of the initial finite perturbation of a homogeneous steady state while the travelling interface separates the domain occupied by irregular spatio-temporal oscillations from the uniform spatial distribution region. The speed of the interface can be found analytically [60].

It should be noted that for somewhat more complex (e.g. nonmonotonic) initial conditions, a system may be characterized by even more complicated dynamics; that is, it may acquire a so-called intermittent structure. Then, the domains occupied by regular and chaotic phases alternate in space (Fig. 3), and the following initial conditions should be considered:

$$u(x,0) = u_* + \varepsilon(x-x_1)(x-x_2)\,, \tag{2.16}$$

$$v(x,0) = v_*\,. \tag{2.17}$$

In this case, slightly disturbed initial conditions evolve into a complex spatial structure in which two domains occupied by sharp patterns separate smooth-patterned regions. Figure 3 shows a snapshot of the species distribution at the moment $t = 600$ calculated for $\varepsilon = 10^{-8}$, $x_1 = 1200$, $x_2 = 2800$ (values of other parameters are the same as in Fig. 1). Similar to the previous case, the size of chaotic domains grows steadily so that they eventually displace the regular phase and occupy the entire region.

The results of our numerical experiments with different types of initial conditions and parameter values indicate

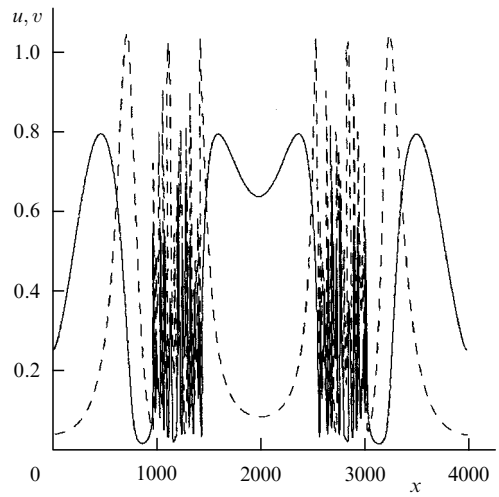

Figure 3. 'Intermittent' spatial structure arising from nonmonotonic initial conditions (2.16), (2.17); see the text for parameters. Solid line — prey, dashed line — predator.

that the formation of clear-cut patterns is normally initiated in the vicinity of the point/points $x_{\rm cr}$, where $u(x_{\rm cr},0) = u_*$, $v(x_{\rm cr},0) = v_*$. Whenever the initial conditions contain no 'critical point', the factors determining the position of the embryo remain unclear.

The pattern formation scenario described in previous paragraphs appears to be essentially different from that known for two-component reaction–diffusion systems [4, 33, 58, 94, 136, 140, 147]. It is worthwhile to note that mathematical model (6), (7) describing the formation of sharp irregular spatial patterns is in a sense minimal because it does not contain common assumptions and constraints, e.g. with respect to relative motions of interacting species or any type of environmental heterogeneity. In the rest of this section, we shall extensively consider this new mechanism of pattern formation. Firstly, we shall present definitive evidence of the chaotic nature of irregular spatio-temporal oscillations described above. Secondly, the results obtained will be extended to the case of a two-dimensional distribution in order to estimate the applicability of this mechanism to the dynamics of natural communities.

2.3 Spatio-temporal chaos

In this section, we show that the formation of clear-cut nonstationary patchy structures in the species distribution corresponds to spatio-temporal chaos. It should be noted that the term chaos has a special meaning, and the apparent irregularity in the system behaviour, no matter how complex it may be, does not necessarily imply chaotic dynamics. By definition, chaos means sensitivity to initial conditions at which small early variations in the distribution of species lead to a large difference at a later time. It has been shown that this characteristic feature of chaos is inseparable from some other properties of system dynamics, such as the specific 'flat' form of Fourier spectra of dynamic variables and exponential decrease of the autocorrelation function [158]. Thus, a variety of methods can be used to reveal chaos.

It is worth noting that the concept of chaos was first elaborated in connection with the temporal dynamics of spatially homogeneous systems. Meanwhile, the dynamics of an extended system may prove much more complex than that and promote the development of chaos in those cases where it

would be otherwise impossible. Specifically, the appearance of chaos in a two-species system is a direct consequence of spatial pattern formation. The phenomenon is essentially a spatio-temporal one; therefore, to distinguish it from a 'purely' temporal chaotic dynamics of homogeneous systems, the term spatio-temporal chaos appears more adequate.

That the formation of sharp temporal patterns corresponds to chaotic dynamics is confirmed by its sensitivity to variations of the initial conditions [264]. As a result, minor changes of the initial conditions account, after a certain time T, for a totally different spatial distribution, regardless of the approach to the numerical evaluation of the difference between perturbed and unperturbed solutions. The dominant Lyapunov exponent corresponding to such chaotic behaviour takes a positive value and is estimated to be $\lambda \cong 0.001$.

Another way to demonstrate the chaotic nature of irregular spatio-temporal oscillations of species abundance is to calculate the autocorrelation function. The state of a predator–prey community is naturally described by two dynamic variables, u and v, defining prey and predator densities respectively. Thus, in the general case, two autocorrelation functions as well as cross-correlations should be considered. The present paper is confined to the results obtained for prey abundance, the autocorrelation function for predator density exhibiting a qualitatively similar behaviour.

It should be noted that the direct application of the standard definition of an autocorrelation function leads to certain problems. In the framework of the usual approach, when the dynamic variable ψ is a function of τ (having the meaning of time or position or any other sense), the autocorrelation function is given by the following expression:

$$F(\xi) = \lim_{Z\to\infty} \frac{1}{Z}\int_0^Z \psi(\tau+\xi)\,\psi(\tau)\,\mathrm{d}\tau\,. \tag{2.18}$$

In the case being considered, prey density depends on two variables, time and position. Therefore, the use of (2.18) to characterize the spatial structure of the system leads to the following expression:

$$\overline{F}(\xi,t) = \lim_{Z\to\infty} \frac{1}{Z}\int_0^Z u(x+\xi,t)\,u(x,t)\,\mathrm{d}x\,. \tag{2.19}$$

Eqn (2.19) has a few evident drawbacks. First, the autocorrelation function calculated from (2.19) depends not only on the distance ξ but also on time. The situation in which the properties of $\overline{F}(\xi)$ are time-dependent looks rather exotic and makes it difficult to interpret the results. On the other hand, the structures under study varying in time, a proper definition of the autocorrelation function should take into account both spatial and temporal behaviour of the system. Another problem is that, in order to obtain reliable results of a computer simulation, the value of Z in Eqn (2.19) must be chosen sufficiently large. In practice, this means that the numerical grid must consist of at least a few tens of thousands of nodes which is hardly feasible.

To overcome these difficulties, we consider a modified definition of the autocorrelation function in which spatial averaging is substituted by averaging over time:

$$K(\xi) = \lim_{T\to\infty} \frac{1}{T}\int_0^T u(x_0+\xi,t)\,u(x_0,t)\,\mathrm{d}t\,. \tag{2.20}$$

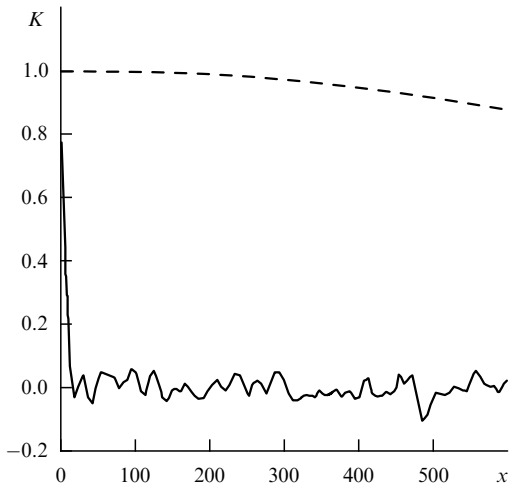

Figure 4. Autocorrelation function $K(\xi)$ calculated for sharp (solid line) and smooth (dashed line) pattern formation regimes.

Note that Eqn (2.20) includes the usual definition as a particular case if the system exhibits an ergodic behaviour. Also, the results of numerical simulation at different x_0 values show no dependence on x_0 although the value of K formally depends on the parameter x_0.

The autocorrelation function $K(\xi)$ calculated in accordance with (2.20) is shown in Fig. 4. The calculations were made at $k = 2.0$, $r = 0.2$, $H = 0.3$, $x_0 = 100$, and the averaging was performed over the time interval from $t = 4000$ to $t = 12000$; the solid line corresponds to a case of irregular (sharp pattern formation) and the dashed line to regular (smooth spatial patterns) dynamics.

To summarize, in the case of a regular dynamics, the spatio-temporal behaviour of the system is highly correlated over the entire domain. Moreover, since the smooth pattern formation regime is in fact a slow relaxation to the uniform spatial distribution, the autocorrelation function gradually changes with time so that the correlation between the temporal behaviour at different points increases. In the infinite time limit, temporal oscillations throughout the system become synchronized and $K(\xi) \equiv 1$.

On the contrary, the behaviour of the autocorrelation function in the case of clear-cut spatial patterns shown in Fig. 4 is typical of chaotic dynamics (cf. [158]). It should be mentioned that irregular oscillations $K(\xi)$ of a finite (non-zero) amplitude (see Fig. 4) result from the finiteness of the averaging interval T; the results of our numerical simulation show that the amplitude tends to zero as T increases. Since the modified definition (2.20) of the autocorrelation function takes into account both temporal and spatial aspects of population dynamics, the dynamic regime corresponding to the formation of sharp spatial patterns can be classified as spatio-temporal chaos. This inference agrees with the recent results of Petrovskii and Malchow (see Ref. [59] where the spatio-temporal chaos in a predator–prey system is described in terms of temporal behaviour of spatially averaged population densities).

2.4 Pattern formation in a two-dimensional case

Now, we consider the extension of the above results to a two-dimensional case. In this case, Eqns (2.6), (2.7) take the

following form:

$$\frac{\partial u(x,y,t)}{\partial t} = \frac{\partial^2 u}{\partial x^2} + \frac{\partial^2 u}{\partial y^2} + u(1-u) - \frac{u}{u+h}\,v\,, \qquad (2.21)$$

$$\frac{\partial v(x,y,t)}{\partial t} = \frac{\partial^2 v}{\partial x^2} + \frac{\partial^2 v}{\partial y^2} + k\,\frac{u}{u+h}\,v - mv\,. \qquad (2.22)$$

In Eqns (2.21), (2.22), $0 < x < L_x$, $0 < y < L_y$. These equations describe the dynamics of an aquatic community in a horizontal layer, the vertical distribution of species within this layer being assumed homogeneous.

Eqns (2.21), (2.22) were solved numerically. The choice of the domain length L_x and width L_y varied in different computer experiments. For the results presented below, $L_x = 900$, $L_y = 300$. The boundary conditions were chosen so as to ensure a zero-flux across the boundary. As above, the type of system dynamics to a certain extent depended on the choice of initial conditions. For a purely uniform initial species distribution, the system remains homogeneous at any time and no spatial pattern emerges. A slight perturbation of the initially homogeneous conditions [the shape of perturbation may differ; cf. Eqns (2.12), (2.13) and (2.14), (2.15)], induces smooth spatial patterns which are unstable and gradually evolve into a uniform spatial distribution. However, somewhat stronger disturbed initial conditions give rise to sharp irregular spatial patterns which persist a long time.

We present here the results of two computer experiments differing in terms of initial conditions. In the first case, the initial distribution of species was given by a two-dimensional generalization of Eqns (2.16), (2.17). Specifically,

$$u(x,y,0) = u_* - \varepsilon_1(x-0{,}1y-225)(x-0{,}1y-675)\,, \qquad (2.23)$$

$$v(x,y,0) = v_* - \varepsilon_2(x-450) - \varepsilon_3(y-150)\,, \qquad (2.24)$$

where $\varepsilon_1 = 2\times10^{-7}$, $\varepsilon_2 = 3\times10^{-5}$, and $\varepsilon_3 = 1.2\times10^{-4}$ (note that the initial conditions were deliberately chosen to be asymmetric in order to emphasize the effect of the corners of the domain in which integration was performed). The values of parameters in Eqns (2.21), (2.22) were taken as $k = 2.0$, $r = 0.3$, $h = 0.4$.

Figure 5 presents snapshots of the species spatial distribution at different times: (a) $t = 0$, (b) $t = 150$, (c) $t = 200$, (d) $t = 300$, (e) $t = 400$, and (f) $t = 1000$. Since both species exhibit a qualitatively similar behaviour (except for early stages of the process influenced by the initial conditions), only the prey (phytoplankton) abundance is shown.

Thus, for the two-dimensional system (2.21), (2.22), the formation of an irregular patchy structure (see Fig. 5f) can be preceded by the evolution of a spiral spatial pattern. The centre of each spiral lies at a certain critical point, i.e. at a point $(x_{\rm cr}, y_{\rm cr})$ where $u(x_{\rm cr}, y_{\rm cr}) = u_*$, $v(x_{\rm cr}, y_{\rm cr}) = v_*$. It is easy to see that the distribution (2.23), (2.24) contains exactly two such points; for different initial conditions, the number of spirals may be different. The spirals having been formed (Fig. 5b), their size slowly increases for some time and the spatial structure becomes more distinct (Figs 5b and 5c). They start to degenerate from the centre (Fig. 5d). The newly-formed 'embryo' of the patchy structure grows steadily (Figs 5d and 5e), and the irregular spatial pattern eventually spreads over the entire domain.

In the second case, the initial conditions describe a phytoplankton (prey) patch placed into a domain with a

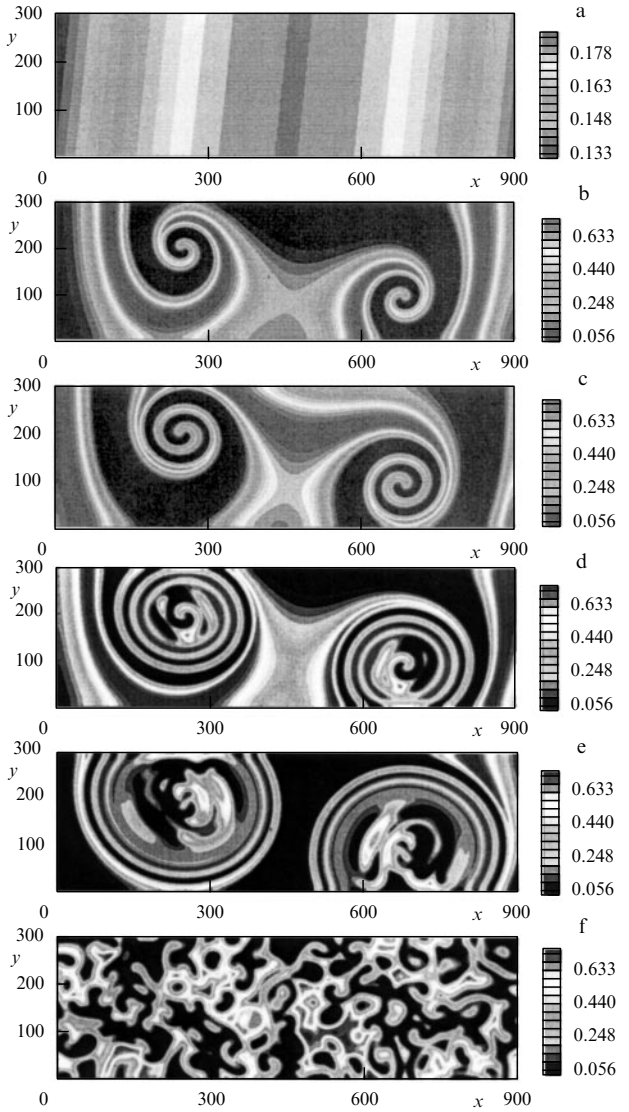

Figure 5. Spatial distribution of prey (phytoplankton) at different times: (a) $t = 0$, (b) $t = 150$, (c) $t = 200$, (d) $t = 300$, (e) $t = 400$, and (f) $t = 1000$; the parameters are given in the text. An irregular patchy structure arises as a result of spiral destruction.

constant-gradient zooplankton (predator) distribution:

$$u(x,y,0) = u_* - \varepsilon_1(x-180)(x-720) - \varepsilon_2(y-90)(y-210)\,, \qquad (2.25)$$

$$v(x,y,0) = v_* - \varepsilon_3(x-450) - \varepsilon_4(y-135)\,, \qquad (2.26)$$

where $\varepsilon_1 = 2\times10^{-7}$, $\varepsilon_2 = 6\times10^{-7}$, $\varepsilon_3 = 3\times10^{-5}$, $\varepsilon_4 = 6\times10^{-5}$.

Figure 6 presents snapshots of the plankton distribution at times (a) $t = 0$, (b) $t = 120$, (c) $t = 160$, (d) $t = 300$, (e) $t = 400$, and (f) $t = 1200$ for the following parameter values: $k = 2.0$, $r = 0.3$, $h = 0.4$. Although in these initial conditions, the system dynamics prior to the formation of a patchy spatial structure is somewhat less regular than in the previous case, it seems to follow a similar scenario. Again, the spirals first appear with their centres at critical points (Figs 6b and 6c) even though their form is not so perfect as before. The destruction of the spirals leads to the formation of two growing embryos of the patchy spatial pattern (Figs 6d and

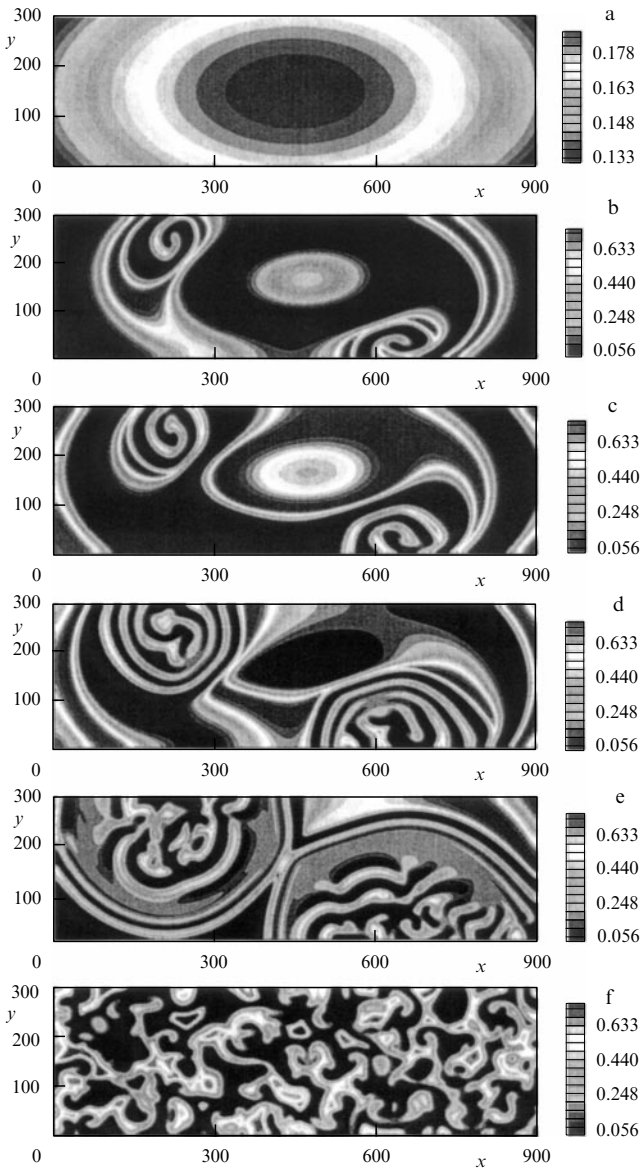

Figure 6. Spatial distribution of prey (phytoplankton) at different times: (a) $t = 0$, (b) $t = 120$, (c) $t = 160$, (d) $t = 300$, (e) $t = 400$, and (f) $t = 1200$; the parameters are given in the text.

6e) and, finally, to the irregular patchy species distribution over the entire integration domain.

It should be emphasized that the formation of a spiral structure in the spatial distribution of plankton may shed new light on some unresolved problems. The existence of dipole-like structures in the plankton distribution in the world's ocean is a well-known phenomenon normally related to the so-called mushroom-like structure of the advective current field [159]. We have shown that such a structure may arise as a result of predator–prey trophic interactions in aquatic communities and need not be necessarily associated with oceanic hydrodynamics.

In conclusion, although the system dynamics appears rather regular at 'intermediate' time scales (Figs 5b and 5c), the evolution of the species spatial distribution may, in the longer run, lead to the formation of an irregular patchy structure (Figs 5e and 5f). These predicted spatial patterns are consistent with the results of field observations on the functioning of planktonic systems (cf. Refs [76, 79, 151, 153]). The relevance of this pattern formation mechanism to the patchy plankton spatial distribution in the marine environment can be evaluated from the analysis of the characteristic size of the arising spatial structures. Taken together, the patterns shown in Figs 5f and 6f and the behaviour of the autocorrelation function $K(\xi)$ (cf. Fig. 4) suggest a characteristic intrinsic length of these structures estimated at 10–25 in dimensionless units. According to Eqns (2.5), the value of this parameter in dimensional units is a function of the maximum phytoplankton growth rate and turbulent diffusivity. The maximum growth rate α undergoes seasonal variations and amounts to $4 \times 10^{-5} - 10^{-5}$ during water bloom periods, corresponding to a doubling time for phytoplankton biomass of 6–48 hours. The effects of turbulent diffusivity are somewhat more complicated. In the open sea, the intensity of turbulent mixing usually depends on the scale of the pattern being examined [92, 160, 161]. In the case of a single plankton patch, the diffusion coefficient may grow with time [162]. However, this property of turbulent mixing is much less manifested in coastal regions, such as bays, harbours, etc., where so-called small-scale turbulence occurs and the diffusion coefficient $D = 10^3\ \mathrm{cm^2\,s^{-1}}$ [160, 163]. It follows from the estimates of D and α and also from Eqn (2.5) that the dimensionless unit length corresponds to approximately 50–100 m in original dimensional units. This gives the intrinsic length of a spatial pattern on the order of 1 km, in agreement with the observed characteristic size of plankton spatial structures [71, 72, 79].

3. Relationship between the formation of plankton spatio-temporal patterns and the cruising of planktivorous fish schools

3.1 Subject-matter of this section

The previous section demonstrated the efficiency of classical continuous two-species models for the description of pattern formation in a planktonic community. However, the continuous approach using ordinary or partial differential equations often fails to account for the individual goal-oriented behaviour of model species in their environment and for their mutual adaptation. This difficulty has been partly overcome in the framework of the concept of complex adaptive systems (first suggested by Holland [164] and further elaborated by modern authors) and simulation strategies for individual behaviour. With this approach, the behaviour of several 'agents' is usually assumed to obey a limited set of strictly defined rules determining the growth, interaction, and motion of these agents and their interplay with the environment. These rules taken on a certain microscale may govern the formation of temporal, spatio-temporal or functional macrostructures.

In the present section, this concept is applied to a dynamic study of a system of fish and plankton populations. A hybrid model simulates the mutual control of continuous spatio-temporal dynamics of two interacting spatially dispersed populations (phytoplankton and zooplankton) and the behaviour of a discrete agent (fish school) subject to given rules. A similar hybrid model was used earlier to describe morphogenesis in cellular tissues [166].

The process of aggregation of individual fish into a school and its persistence under environmental or social constraints have been studied by many authors [23, 25, 167–178] and will not be considered here.

It is important to note that predator – prey relationships form the basis of any food chain. At the same time, this concept was employed in the Marxist class struggle models likening the employment rate to a prey and the wages to a predator (see Ref. [180]). Also, the relationship between economic and ecological factors equally well applies to fishery [181].

3.2 Model of a 'nutrient – plankton – fish' system

3.2.1 Continuous plankton dynamics. We consider a four-component 'nutrient – phytoplankton – zooplankton – fish' model in which phytoplankton $P(X, Y, \tau)$ and phytophagous zooplankton $H(X, Y, \tau)$ population dynamics at any point (X, Y) and time τ are given by the following reaction – diffusion equations:

$$\frac{\partial P}{\partial \tau} = RP\left(1 - \frac{P}{K}\right) - \frac{AC_1 P}{C_2 + P} H + D_P \Delta P\,, \tag{3.1}$$

$$\frac{\partial H}{\partial \tau} = \frac{C_1 P}{C_2 + P} H - MH - F\frac{H^2}{C_3^2 + H^2} + D_H \Delta H\,. \tag{3.2}$$

Parameters R, K, M, and $1/A$ denote the intrinsic growth rate and carrying capacity of phytoplankton, the mortality and nutrient assimilation rates of zooplankton respectively. Constants C_1, C_2, and C_3 parameterize the saturating functional response of zooplankton; F is the fish predation rate on zooplankton; D_P and D_H are the diffusion coefficients of phytoplankton and zooplankton respectively; Δ is the two-dimensional Laplace operator. A change in phytoplankton biomass resulting from its consumption by zooplankton is a type II functional response whereas fish predation on zooplankton is described by a type III sigmoid functional reaction, in agreement with the assumptions of the Scheffer model [44].

The local kinetics of the model, i.e. $D_P = D_H = 0$, have been considered in detail in Refs [41, 44]. In the absence of zooplankton, phytoplankton would reach its carrying capacity K. By considering zooplankton as a non-dynamic predator, on condition that $\partial H/\partial \tau = 0$, it is easy to show the existence of two stationary phytoplankton levels if zooplankton densities are not too high. In contrast, high zooplankton density is associated with a single stable low phytoplankton level and vice versa. Dynamic zooplankton can induce typical predator – prey limit cycle oscillations, and the introduction of effects exerted by zooplanktivorous fish with the last kinetic term in Eqn (3.2) restores bistability. Which of the two stationary states is reached depends on the initial conditions provided neither external nor internal noise interferes. Fluctuations due to natural noise as well as 'extreme' events can induce transitions between the stationary states.

The behaviour of a local model subjected to seasonal changes has been studied in Refs [45, 71, 72]. Such seasonal impacts may be due to natural variations of temperature, light, and nutrient supply. The local predator – prey limit cycles can transform to quasi-periodic and chaotic oscillations while locally stable states simply oscillate with an externally-induced frequency.

Considering diffusion allows diffusion-induced plankton patchy distributions to be revealed which remain stable despite weak seasonal effects [46]. However, such spatial structures arise only if prey and predator populations are characterized by different diffusion coefficients [4, 33]. In the case of their having similar diffusivity, time-related changes in the patch distribution occur if the instability of uniform plankton patterns is due to growth, interactions, diffusion, and advection [141] or if certain parameters, e.g. nutrient concentration, show a spatial gradient [58].

Hydrodynamic forces and the spatio-temporal flow patterns they induce frequently drive or restrict structures formed by drifting and floating matter. Hydrodynamic processes are usually much faster than biological ones in plankton communities. This allows a method for the separation of variables [147] to be employed which is beyond the scope of the present paper. This section deals with physically uniform pieces of time and space.

For convenience, the model (3.1), (3.2) is simplified by the introduction of dimensionless densities $p = P/K$ and $h = AH/K$ as in Pascual's work [58]. Space is scaled by a characteristic length L/k equalling the total length L of the area under consideration divided by an integer factor k which determines the scale of the expected patchy patterns. Time is scaled by the characteristic phytoplankton growth rate R_0. Hence,

$$x = \frac{kX}{L}\,, \qquad y = \frac{kY}{L}\,, \qquad t = \tau R_0\,.$$

In this case, Eqns (3.1), (3.2) are converted to

$$\frac{\partial p}{\partial t} = rp(1 - p) - \frac{ap}{1 + bp} h + d_p \Delta p\,, \tag{3.3}$$

$$\frac{\partial h}{\partial t} = \frac{ap}{1 + bp} h - mh - f\frac{gh^2}{1 + g^2 h^2} + d_h \Delta h\,, \tag{3.4}$$

where the new parameters are

$$r = \frac{R}{R_0}\,, \qquad a = \frac{C_1 K}{C_2 R_0}\,, \qquad b = \frac{K}{C_2}\,, \qquad m = \frac{M}{R_0}\,,$$

$$f = \frac{F}{C_3 R_0}\,, \qquad g = \frac{K}{C_3 A}\,, \qquad d_p = \frac{k^2 D_P}{L^2 R_0}\,, \qquad d_h = \frac{k^2 D_H}{L^2 R_0}\,.$$

The results reported in this work have been obtained by numerical simulation for a set of parameters $r = 2$, $a = 5$, $b = 5$, $m = 0.6$, $g = 2.5$ chosen so as to have limit cycles at each point under $f = 0$.

It is frequently supposed that in natural waters the plankton diffusion rate is a function of turbulent diffusion. With this in mind, both phytoplankton and zooplankton may be regarded as a passive admixture transported by turbulent water flows [182 – 185]. Therefore, $d_p = d_h = d$. Using the relationship between the turbulent diffusion and the spatial scale of the phenomenon of interest in the open sea [92, 161], it can be shown that, at the characteristic growth rate $R_0 = 10^{-5}$ s^{-1} (or one division per day as is typical of phytoplankton propagation) and the characteristic length $L/k = 1$ km (typical of plankton spatial patterns), d is about 5×10^{-2}.

Numerical integration of Eqns (3.3), (3.4) was performed using a simple difference scheme. The two-dimensional space was divided into a rectangular grid of 64×64 quadratic finite elements of unit length each. The time step was set equal to 0.01. Repeated integration at a smaller step showed that the numerical results are independent of its size and thus confirmed the accuracy of the adopted approximation.

Periodic boundary conditions were chosen for both spatial directions.

3.2.2 Discrete fish school dynamics. It is generally accepted that the predation rate of planktivorous fish is a constant parameter in plankton-fish interaction models [44, 55, 70]. This implies that fish must always be uniformly distributed in space. But it is well known that fish can form mobile schools. For such fish schools occupying spatially confined regions, f is not a constant but is a function of zooplankton density h, time t, and space (x, y); i.e. in Eqn (3.2), $f = f(h, t, x, y)$. Function f describes the plankton density-dependent travelling of a fish school to a region favourable in terms of food availability. Such a motion can be simulated in a variety of ways [167, 186].

In this paper, we suggest that the behaviour of a fish school obeys the rules formulated by Ebenhöh [187]. In this case, a localized fish school moves, in search of food, to the nearest region with highest concentration only after the local zooplankton density is reduced (as a result of predation) to or below a certain threshold value h_{th} and the density gradient across the border of the habitat becomes higher than a threshold δh_{th}. This, however, does not occur before some residence time τ_{th} has elapsed.

The Ebenhöh rules reflect observations of fish school movements in natural waters [167, 187–189]. However, the rules are simplified on the assumption that fish schools travel independently of one another other and their specific characteristics (e.g. size, speed, and residence time) remain unaltered. The model (3.3), (3.4) with function f describing fish school movements following the Ebenhöh automata rules combines the characteristic features of a cellular automaton and a model based on partial differential equations.

Fish movements were calculated taking into account the Ebenhöh rules. The fish predation rate on zooplankton $f_{ij}^{(n)}$ was assumed to equal f_0 if the school was in position (i, j) at a time step $n\delta t$; otherwise, the predation rate was zero. The resulting zooplankton density gradient was computed numerically by the formula

$$(\boldsymbol{\xi}\nabla h)_{ij}^{(n)} = |\xi_x|\, h_{i+\operatorname{sign}(\xi_x),\, j}^{(n)} + |\xi_y|\, h_{i,\, j+\operatorname{sign}(\xi_y)}^{(n)} - h_{ij}^{(n)} . \quad (3.5)$$

3.3 Formation of spatial plankton patterns resulting from fish school motions

Figure 7 demonstrates phytoplankton and zooplankton spatial patterns that emerge as a result of the fish-plankton interplay. It can be seen that the phytoplankton density falls in the regions where zooplankton is abundant and vice versa. Many early observers reported an inverse relationship between phytoplankton and zooplankton densities [71]. Obviously, this is due to the consumption of the former by the latter. As a result, the penetration of phytoplankton into the regions occupied by zooplankton is blocked.

Spiral waves generated by phytoplankton and zooplankton are shown in Fig. 7. Two and three-dimensional spiral waves are known to emerge in excitable physical, chemical, and biological media [190–194]. For example, they play an important role in heart rhythm disturbances and in biomorphogenesis. In the ocean, they look like rotary motions of plankton patches on a kilometer scale [111]. The formation of such waves has been described in detail in Refs [183, 266]. It has been shown that these spirals are stable over 10^6 iterations equivalent to more than 50 real time years. However, they proved sensitive to physical perturbations, such as shear flows [195] and nutrient gradients [182].

Interestingly, fish school mobility falls dramatically at a low predation rate f of zooplankton-eating species, and spiral waves do not appear. Instead, point sources arise in this case (Fig. 8).

The formation of both spiral waves (see Fig. 7) and point sources (see Fig. 8) is followed by a sharp decrease of

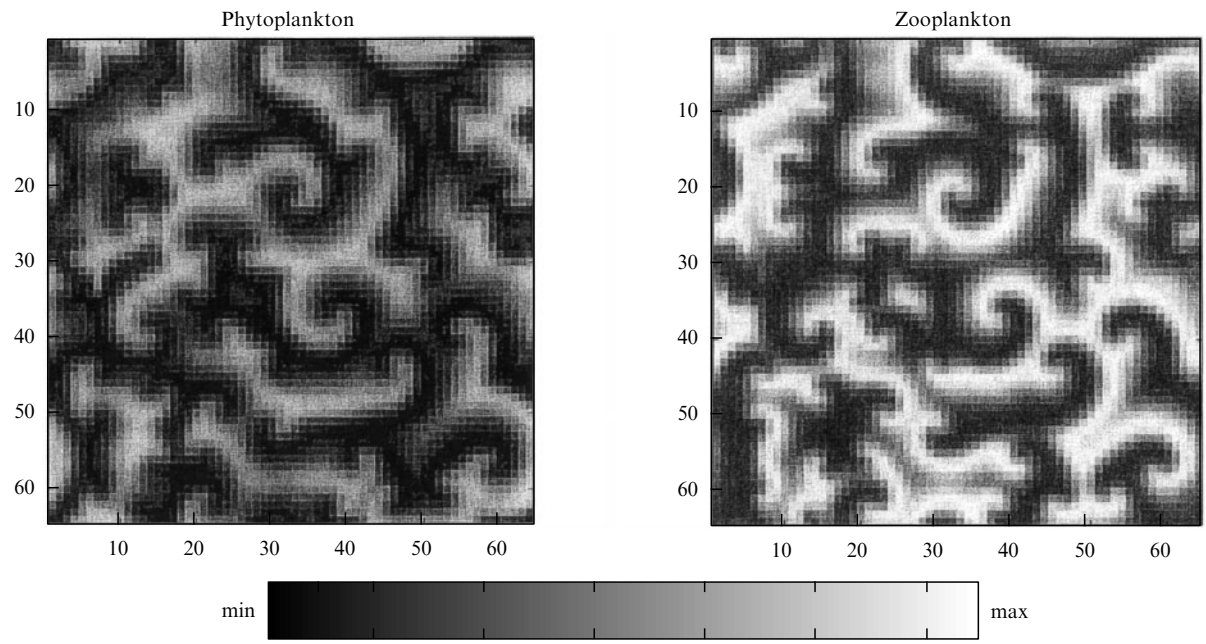

Figure 7. Phytoplankton and zooplankton spatial distribution obtained in model (3.3), (3.4). The density scale is shown at the bottom of the figure; $f = 2$.

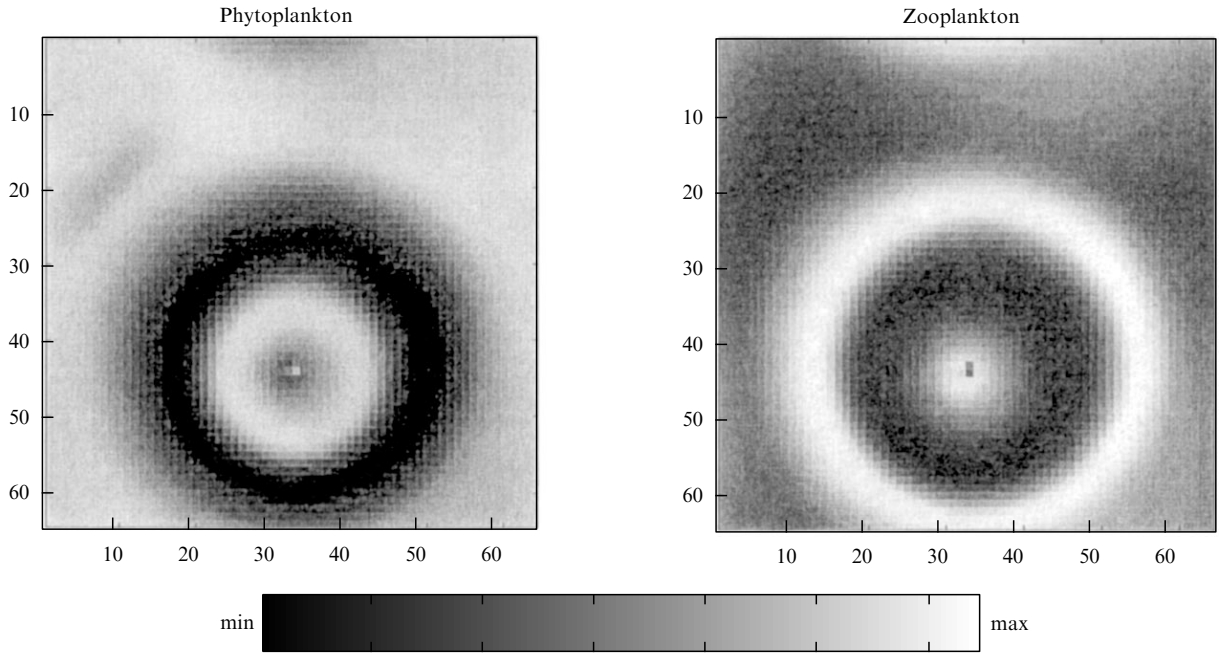

Figure 8. Plankton waves emitted by a point source at $f = 1$. The density scale is shown at the bottom of the figure.

spatially-averaged plankton density oscillations

$$\langle p \rangle = \frac{1}{S}\int_{(S)} p(x, y, t)\,\mathrm{d}x\,\mathrm{d}y\,, \qquad \langle h \rangle = \frac{1}{S}\int_{(S)} h(x, y, t)\,\mathrm{d}x\,\mathrm{d}y\,, \tag{3.6}$$

where $S = k^2$, $k = 64$. It turned out that plankton density oscillations at $f = 1$, unlike those at $f = 2$, display aperiodic bursts coincident with drastic changes of fish school location (Fig. 9).

It may be concluded that plankton dynamics depends on fish school movements [183]. Therefore, the analysis of these motions is of practical interest for the studies of plankton – fish interactions.

3.4 Fish school random walks resulting from the fish-plankton interplay

3.4.1 Regularity of irregular walks. Fish school motions are controlled by various biotic and abiotic factors, such as light, temperature, salinity, nutrient supply (e.g. plankton density), etc. [167, 186]. On the other hand, fish school walks have been shown to depend on plankton – fish interactions [167, 183, 187, 189] which in turn influence plankton dynamics [183]. It is no wonder that school movements governed by the interplay between fish and their environment may be highly irregular [183, 184].

An irregular behaviour exhibits very erratic features and is described by irregular functions. The irregular functions may be (1) selfaffine and (2) multiaffine. If function (F) represents a stochastic process, it may be given by the following formulas [196 – 199]:

$$\left\langle \left| F(x + l) - F(x) \right| \right\rangle \sim l^{H} \tag{3.7}$$

(where $\langle \ldots \rangle$ means averaging) for case (1) and

$$\left| F(x + l) - F(x) \right| \sim l^{h(x)} \tag{3.8}$$

for case (2). The exponent H in Eqn (3.7) is called the *Hurst exponent*. Note that if $H < 1$, then F is not differentiable, and the smaller H the more singular is F. Thus, the Hurst exponent characterizes the degree of global irregularity of function F. Exponent $h(x)$ in Eqn (3.8) is called the *Holder exponent*. It is a measure of F irregularity at point x. The greater the Holder exponent the more regular the function F. Selfaffine and multiaffine functions are regarded as fractal and multifractal respectively [198 – 200]. The latter are characterized by a multifractal spectrum $D(h)$ that describes the distribution of Holder exponents and represent the Hausdorff dimension of such a subset for which the Holder exponent is h:

$$D(h) = \dim_{\mathrm{H}} \left[x \middle| \, h(x) = h \right] , \tag{3.9}$$

where, in the general case, h may have either a positive or negative value [198, 200, 201].

Multifractal processes can also be characterized by a singularity spectrum $f(\alpha)$ which relates the Hausdorff dimension of $f(\alpha)$ to a subset carrying measure μ with the singularity strength α:

$$f(\alpha) = \dim_{\mathrm{H}} \left[x \middle| \, \mu\big(B_x(\varepsilon)\big) \right] , \tag{3.10}$$

where $B_x(\varepsilon)$ is the ε-box centred at x, and

$$\mu\big(B_x(\varepsilon)\big) \sim \varepsilon^{\alpha(x)} . \tag{3.11}$$

Homogeneous measures are characterized by a singularity spectrum given by a single point $\big(\alpha_0, f(\alpha_0)\big)$. In other words, only one kind of singularity is inherent in the measure. Multifractal measures involve singularities of different strengths. Generally speaking, the approach based on the $f(\alpha)$ spectrum of singular measures has the same status as that based on the Holder exponent spectrum $D(h)$ [201].

The question arises of whether fish school movements can be described by simple equations (3.7) or (3.8) and, if so, which of the two provides the best fit to such movements.

3.4.2 Fish school trajectories. A fish school obeying the Ebenhöh rules travels to the regions with the highest

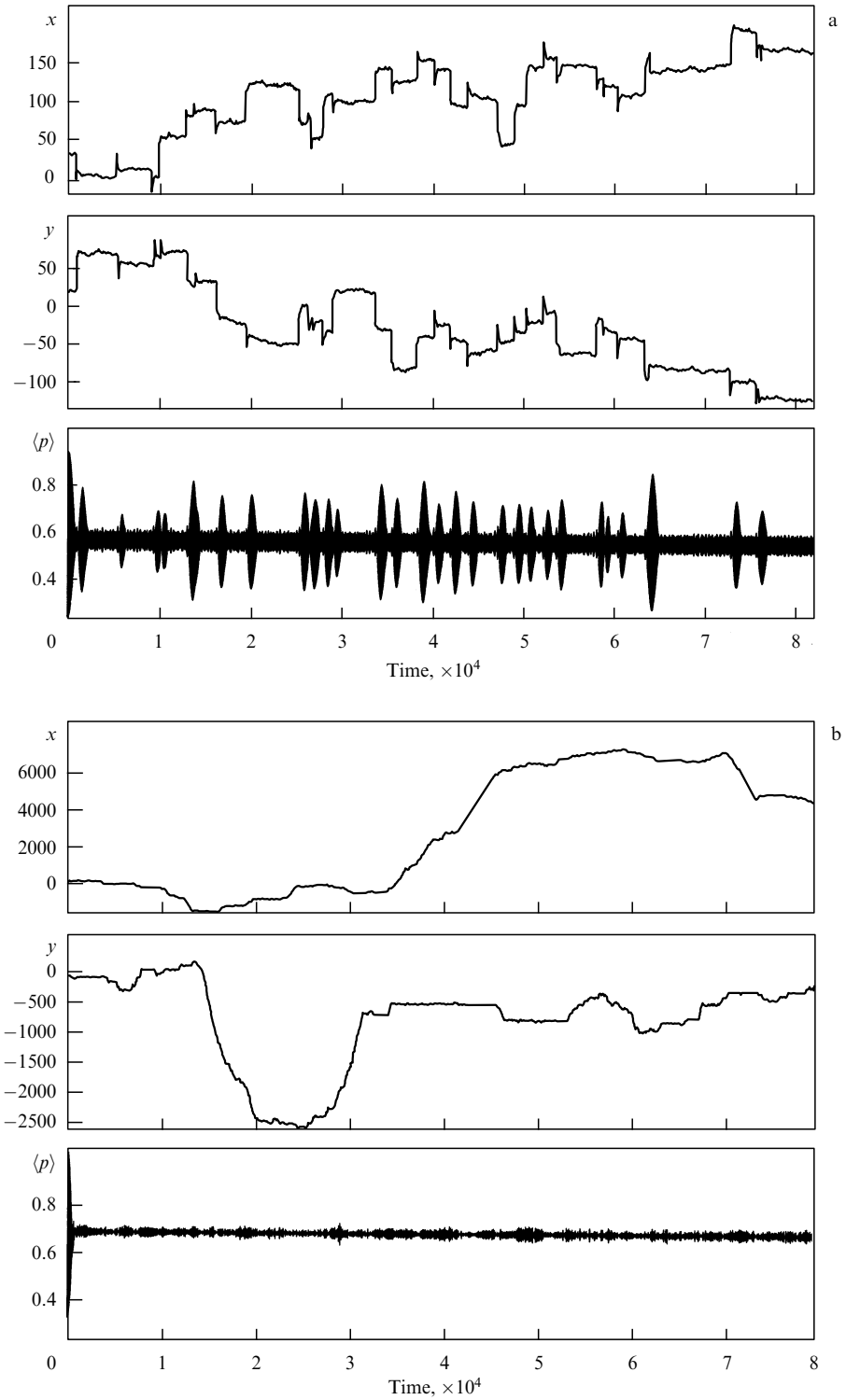

Figure 9. (a) x and y projections of fish school movements and averaged phytoplankton density $\langle p \rangle$ oscillations at $f = 1$. (b) x and y projections of fish school movements and averaged phytoplankton density $\langle p \rangle$ oscillations at $f = 2$. Averaged zooplankton density $\langle h \rangle$ oscillations (not shown) are phase shifted and qualitatively similar to averaged phytoplankton density oscillations.

zooplankton density. Since the plankton distribution changes with time, the walks of the school are somewhat chaotic. Figure 10 demonstrates typical fish school trajectories, both highly (at $f_0 = 1$) and poorly (at $f_0 = 15$) persistent. In either case, $h_{\text{th}} = 0.35$, $\delta h_{\text{th}} = 0.01$, and $\tau_{\text{th}} = 0.08$.

Evidently, the transition from low to high fish predation rate markedly reduces the persistence of fish school movements; indeed, the school retains the direction of its motion at $f_0 = 1$ much longer than at $f_0 = 15$. A more subtle analysis of school walks reveals characteristic features of either type of fish behaviour.

3.4.3 Multifractal analysis of fish school walks. Recently, we have shown that fish school walks can be regarded as fractal Brownian motion with the Hurst exponent H depending on both the phytoplankton growth rate and the fish predation

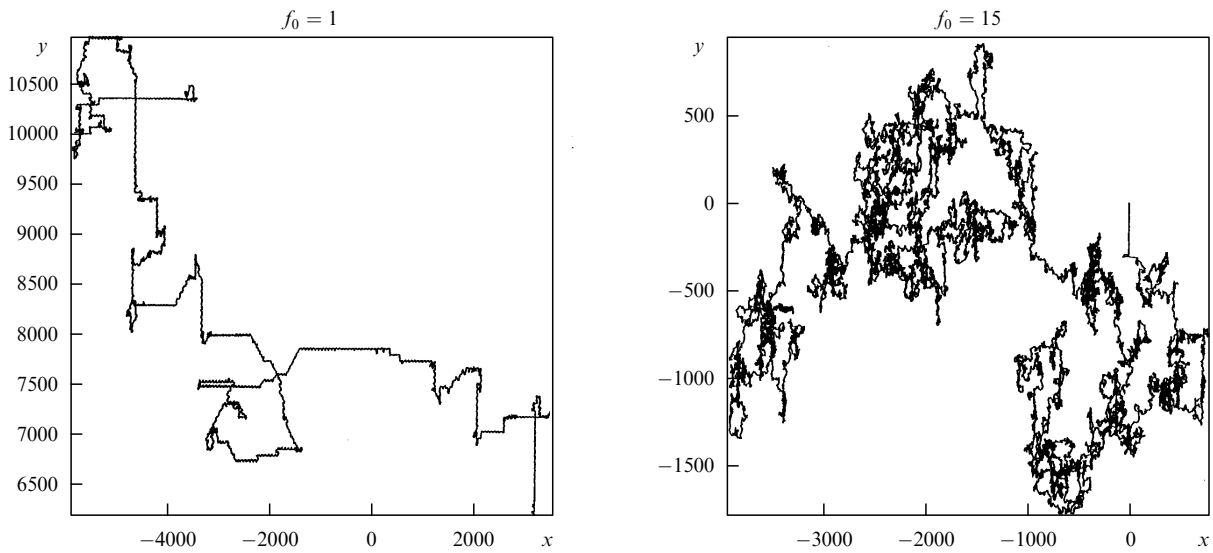

Figure 10. Fish school walks at different f_0 values (shown above each trajectory) for which plankton spatial distributions presented in Fig. 7 are taken as initial. In the course of time, these distributions undergo no qualitative changes (see Ref. [183] for more details).

rate on zooplankton [183, 185]. However, caution is needed when using the Hurst exponent in the analysis of Brownian signals because this approach tends to yield imprecise estimates of H when the function of interest is not a spatially homogeneous fractal function with constant 'roughness' described by the exponent H [202].

In the present paper, it is not supposed *a priori* that a fish school trajectory can be represented by a spatially homogeneous fractal function; rather, we carry out the multifractal analysis of fish school walks (cf. Ref. [184]). A strategy is used which provides a practical possibility to directly derive singularity spectra $D(h)$ (3.9) and $f(\alpha)$ (3.10) from any experimental signal [201, 203, 204]. This approach is essentially that of transformations used in the 'wavelet (burst) theory' [76, 77, 205–208, 266]. It includes a space-scale analysis which consists of expanding signals in terms of the so-called wavelets constructed, by means of translations and dilations, from a certain single function referred to as the *analysing wavelet* ψ. The continuous wavelet transform of a real-valued function F is defined as

$$W_\psi[F](b,a) = \frac{1}{a}\int_{-\infty}^{+\infty} F(x)\,\psi\left(\frac{x-b}{a}\right)\mathrm{d}x\,, \tag{3.12}$$

where b and a are the space and scale parameters respectively. The analysing wavelet ψ is usually chosen to be localized in both space and frequency. The main advantage of wavelet transforms for the analysis of function F regularity is that they 'do not recognize' a signal described by a polynomial function, given a proper choice of the analysing wavelet ψ. The analysing wavelet referred to as the 'Mexican hat', by virtue of its specific shape, will be used throughout this section.

The fastest way to estimate functions $D(h)$ (3.9) and $f(\alpha)$ (3.10) is to analyse the scaling behaviour of the partition function $Z(q,a)$ from the wavelet transform maxima modulus [203]

$$Z = \sum_{i=1}^{N(a)} \big(\omega_i(a)\big)^q\,, \tag{3.13}$$

where $i = 1,\ldots,N(a)$; $N(a)$ is the number of local $W_\psi[F](b,a)$ maxima on each scale a considered as a function of x; function $\omega_i(a)$ can be defined in terms of wavelet transform coefficients [201, 203] as

$$\omega_i(a) = \max_{\substack{(x,a')\in l_i\\ a'\leqslant a}} \big|W_\psi[F](x,a')\big|\,, \tag{3.14}$$

$l_i \in L(a)$; $L(a)$ is a set of lines connecting the wavelet coefficient maxima which reach or cross a level corresponding to scale a.

In the limit $a \to 0^+$, the partition function $Z(q,a)$ exhibits a power law behaviour:

$$Z(q,a) \sim a^{\tau(q)}\,. \tag{3.15}$$

The spectrum $f(\alpha)$ (3.10) can be found by the Legendre transformation, i.e.

$$f(\alpha) = \min_q \big(q\alpha - \tau(q)\big)\,. \tag{3.16}$$

Because $\tau(q)$ is normally differentiable, and $\tau''(q) \leqslant 0$, it is found that

$$\alpha(q) = \frac{\mathrm{d}\tau(q)}{\mathrm{d}q}\,, \tag{3.17}$$

$$f(q) = q\,\alpha(q) - \tau(q)\,. \tag{3.18}$$

Unfortunately, the computation of the Legendre transform has several disadvantages (related, for example, to the local violation of the inequality $\tau''(q) \leqslant 0$). This may lead to errors [209]. Therefore, another approach was developed to derive singularity spectra in the context of the so-called canonical method [209]. It uses the following functions:

$$h(a,q) = \frac{1}{Z(a,q)}\frac{\partial Z(a,q)}{\partial q}\,, \tag{3.19}$$

where

$$\frac{\partial Z}{\partial q} = \sum_{i=1}^{N(a)} \omega_i(a)^q \ln\omega_i(a)\,, \tag{3.20}$$

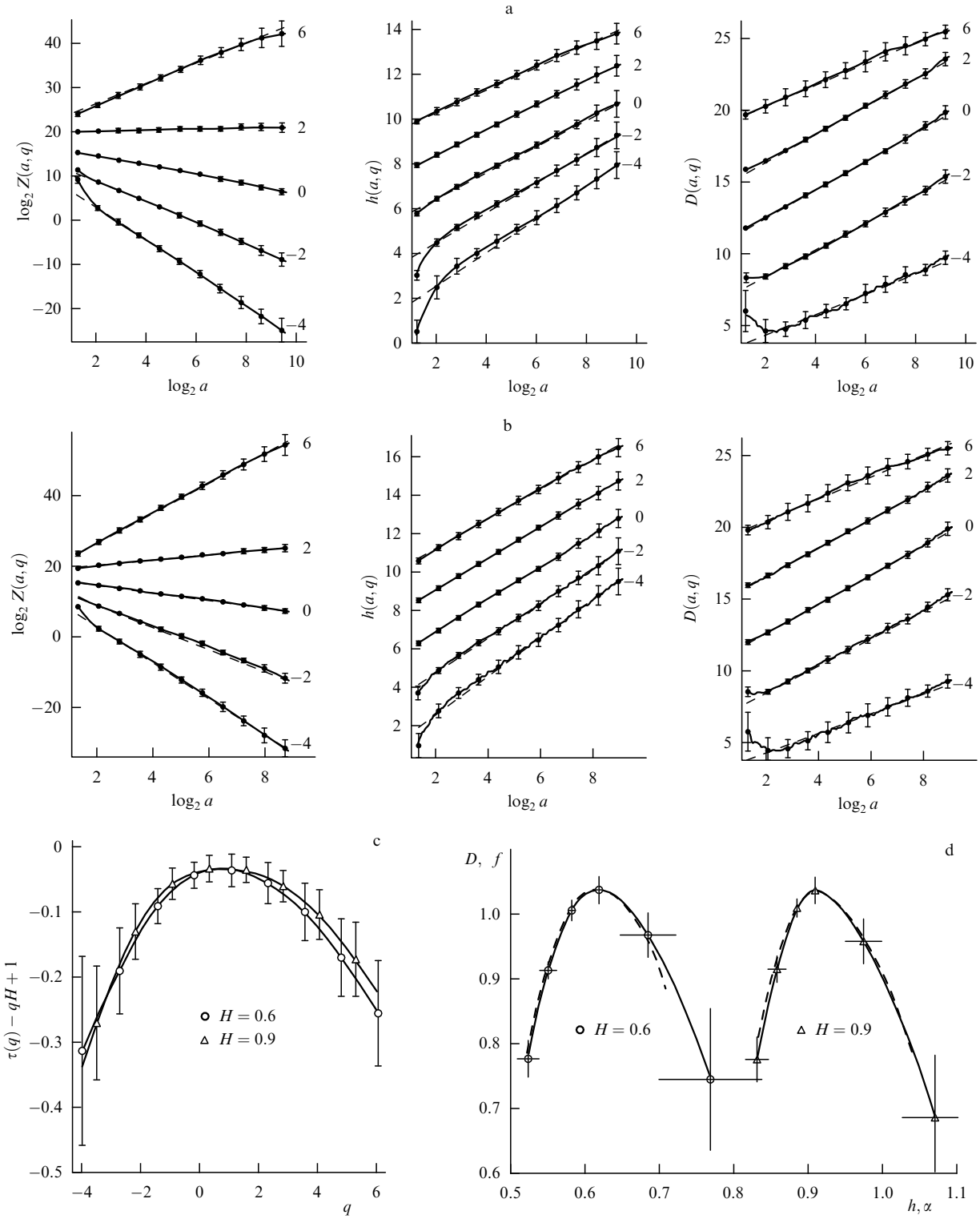

Figure 11. Multifractal analysis of realizations of fractional Brownian processes for (a) $H = 0.6$ and (b) $H = 0.9$. Dependences of $\log_2 Z(a,q)$ on $\log_2 a$, $h(a,q)$ on $\log_2 a$, and $D(a,q)$ on $\log_2 a$ for each process were obtained from 32 realizations, 2^{12} in length each. q values are shown at each graph. (c) The difference between the numerically obtained $\tau(q)$ [Eqn (3.15)] and its theoretical value $\tau(q) = qH - 1$ [201]. (d) $f(\alpha)$ and $D(h)$ spectra (dashed and solid lines respectively).

and, by analogy with Eqn (3.18),

$$D(a,q) = qh(a,q) - \ln Z(a,q)\,. \tag{3.21}$$

$D(q)$ and $h(q)$ spectra are found in the following way [204]:

$$D(q) = \lim_{a\to 0} \frac{D(a,q)}{\ln a}\,, \tag{3.22}$$

$$h(q) = \lim_{a\to 0} \frac{h(a,q)}{\ln a}\,. \tag{3.23}$$

The singularity spectrum $D(h)$ can be computed from Eqns (3.22) and (3.23). Unlike the Legendre transform (3.17), (3.18), this approach makes it possible to avoid any instability related to numerical differentiation and attendant

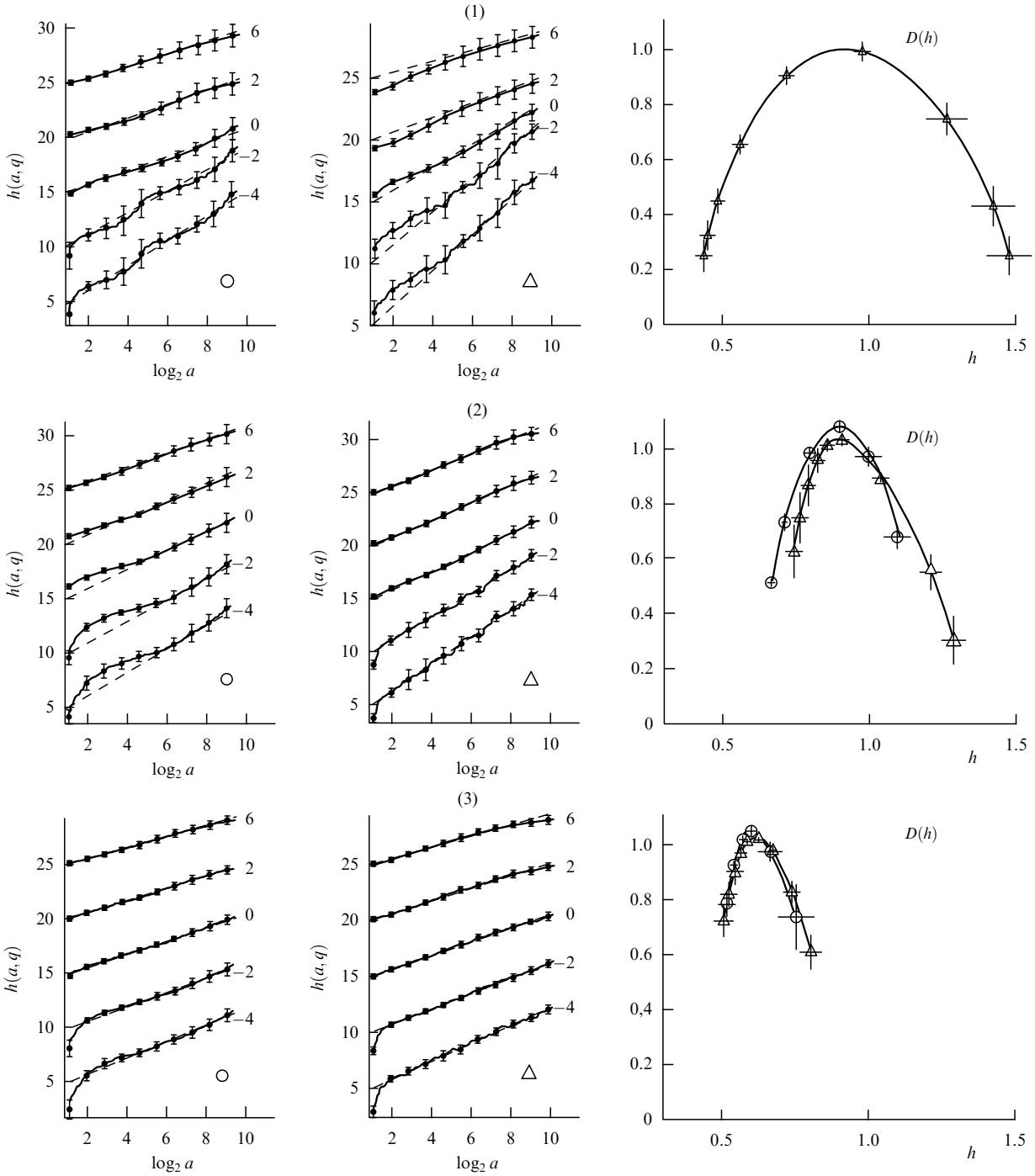

Figure 12a. Multifractal analysis of small-scale (○) and medium-scale (△) fish school walks at different fish predation rates on zooplankton: (1) $f_0 = 1$, (2) $f_0 = 4$, and (3) $f_0 = 15$. Small and medium-scale walks were obtained by splitting fish school trajectories (similar to those in Fig. 10) into sections of length 2^3 and 2^5 respectively. Functions $h(a,q)$ vs $\log_2 a$ and spectra $D(h)$ are presented for each f_0 value (q values are shown on each graph).

errors. At the same time, the canonical method allows one to identify and evaluate errors in the calculation of $D(q)$ and $h(q)$ from the variances in the slope of linear approximations (3.22) and (3.23).

Figure 11 demonstrates how the two approaches work when applied to the model realization of fractional Brownian motion. It can be seen that all functions, $\log_2 Z(a,q)$ vs $\log_2 a$, $h(a,q)$ vs $\log_2 a$, $D(a,q)$ vs $\log_2 a$, are essentially linear in agreement with Eqns (3.15), (3.23), and (3.22) respectively. Note (Fig. 11c) that the difference between the numerical and theoretical values of $\tau(q)$ is virtually independent of H and remains close to zero over rather a wide range of q values. This region widens as the length of realization increases while the error grows with increasing $|q|$. Because the difference between numerical and theoretical values of τ remains nonzero for any finite realization, neither $D(h)$ nor $f(\alpha)$ is a pointlike fractal spectrum. Instead, they form bell-shaped functions the half-width of which is rather small compared with that characteristic of any multifractal process.

Similarly narrow fractal-like spectra are typical of fish school cruising associated with a fish predation rate $f_0 = 15$ [Figs 12a(3)]. It can be seen that $h \approx 0.6$ corresponds to the

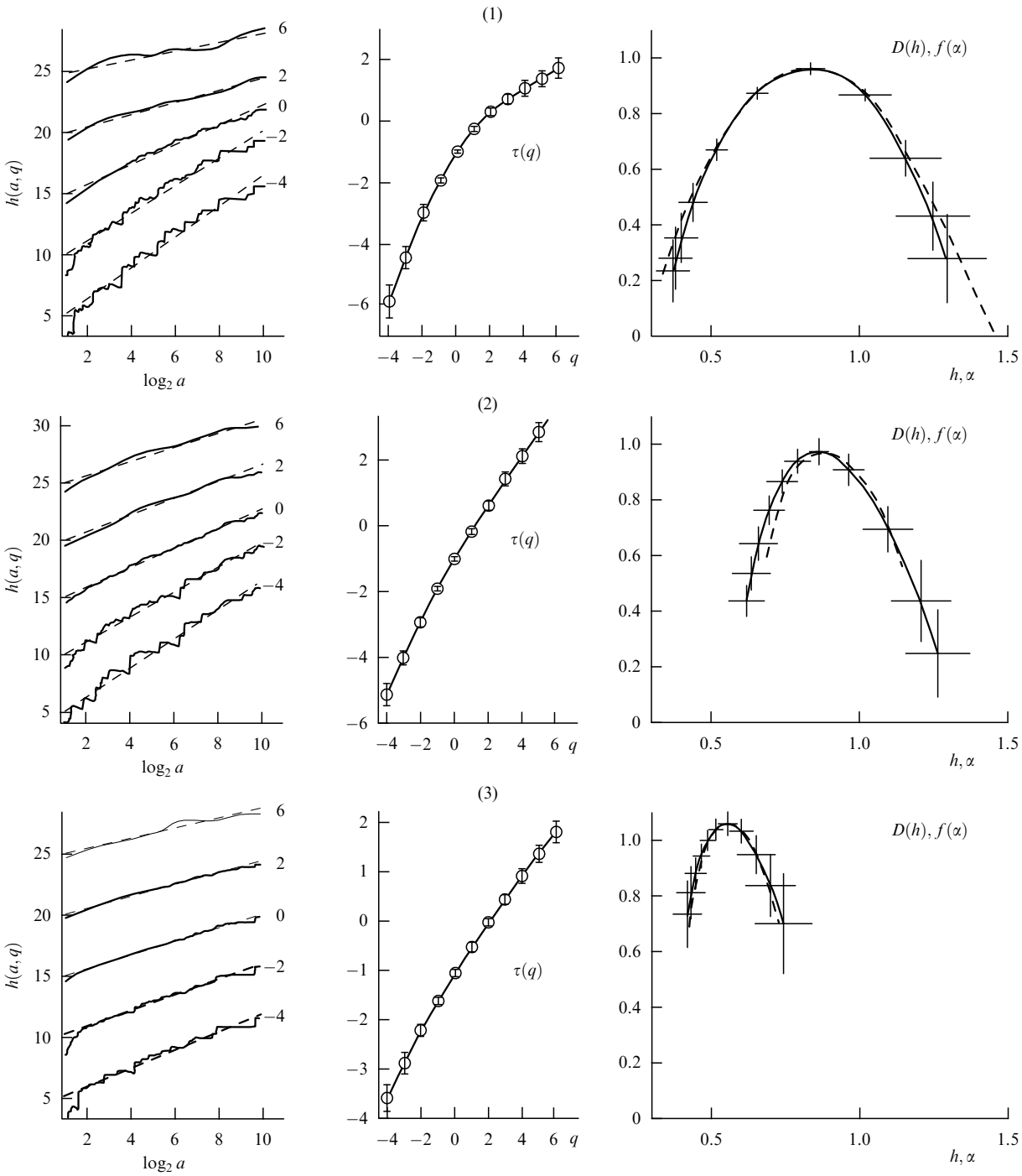

Figure 12b. Multifractal analysis of large-scale fish school walks for different fish predation rates on zooplankton: (1) $f_0 = 1$, (2) $f_0 = 4$ and (3) $f_0 = 15$. Large-scale walks were also obtained by splitting fish school trajectories (similar to those of Fig. 10) of lengths 2^{19} (for $f_0 = 4$ and $f_0 = 15$) and 2^{20} (for $f_0 = 1$) into separate sections of length 2^9. For each value of f_0 the function $h(a, q)$ of $\log_2 a$ (the value of q is shown by each curve), $\tau(q)$, the spectrum $f(\alpha)$ (dashed line) and $D(h)$ (solid line) are shown.

maximum of D. Hence, these movements may be regarded as fractional Brownian motion with the Hurst exponent H, in excellent agreement with the results reported in Ref. [183]. A dramatic change in singularity spectra occurs as f_0 decreases.

Figure 12a(2) presents singularity spectra obtained for small and medium-scale walks of a fish school at $f_0 = 4$. These spectra are broader than in Fig. 12a(3) and have a shape similar to that typical of multifractal spectra [201–204].

Figure 12a(1) demonstrates selected results of multifractal analysis of small and medium-scale fish school walks at $f_0 = 1$. It follows that small-scale motions are characterized by essentially non-linear $h(\log_2 a)$ dependences. As a result, the singularity spectrum cannot be obtained. A spectrum of medium-scale walks is also presented. It is multifractal.

Finally, Fig. 12b shows the results of multifractal analysis of large-scale fish school walks. Evidently, the function $\tau(q)$ for the fractal motion [Fig. 12b(3)] is virtually linear whereas the transition to multifractal spectra $D(h)$ and $f(\alpha)$ is accompanied by the growing non-linearity of function $\tau(q)$. Such non-linearity is typical of multifractal patterns and processes [198].

3.4.4 Concluding remarks. This section presented a hybrid model describing the continuous spatio-temporal dynamics of phytoplankton and zooplankton as well as the discrete dynamics of planktivorous fish. Also, it considered the plankton patch formation known to occur under natural conditions [52, 167, 186]. Fish and plankton dynamics undergo continuous mutual adaptation. Fish school trajectories are strongly dependent on the predation rate f of plankton-eating species (see Fig. 10). Any decrease of f results in a transition from low-persistent to high-persistent fish school movements. The former exhibit fractal properties while the latter are multifractal on large scales. Therefore, seasonal changes of $D(h)$ and $f(\alpha)$ spectra are of practical interest. It can be expected that future experiments and field observations will show whether fish school movements may be characterized in this way.

In conclusion, these results indicate that rather a simple conceptual minimal model (3.3), (3.4) can describe a large variety of fish school movements and the formation of complex plankton spatio-temporal patterns resulting from predator – prey interactions and diffusion processes.

4. Inhomogeneous marine environment

In the preceding section, the plankton system dynamics was mainly considered on the assumption that the properties of the environment are time and space-independent. Strictly speaking, this is not true of the marine environment. The majority of hydrophysical factors controlling the function of a biological community, e.g. temperature, salinity, turbulent mixing, etc., are functions of t and r. This accounts for the appearance of spatial patterns in an aquatic community induced by heterogeneous hydrophysical and hydrochemical fields. To better understand the dynamics of an aquatic community in a real marine environment, it is important to distinguish between 'intrinsic' patterns, i.e. patterns arising from trophic interactions within the community (like those described above), and 'imposed' ones which are due to the heterogeneous environment. The physical nature of environmental heterogeneity (thus, the dispersion of varying parameters and characteristic temporal and spatial scales) can differ considerably from one situation to another. To assess the applicability of the 'homogeneous' models considered above and obtain the information necessary for their further development (to ensure a more realistic approach taking into consideration environmental heterogeneity), we briefly describe the main types of spatial inhomogeneities known to occur in the ocean. This concise and rather schematic account should be considered as an introduction to the subject rather than a comprehensive review. Readers interested in more details are referred to the voluminous scientific literature on this and related issues. Here, this problem is treated in so far as it is necessary for the purpose of this paper.

Before considering concrete cases of hydrophysical heterogeneity, it appears useful to outline the scope of processes that may be of special interest for the further discussion. First of all, it should be borne in mind that the ocean is a highly stratified system characterized by a distinct vertical and horizontal asymmetry. Because we are mainly interested in phenomena arising from the interplay between physical and biological processes, this section is largely concerned with the dynamics of the upper 'productive' sea layer. Being dependent on a number of factors, such as geographic region and season, its thickness has been estimated to vary from tens to hundreds of meters. Since the spatial biological patterns considered in the preceding sections normally arise on scales from hundreds of meters to a few kilometers, they appear to be in the first place related to the horizontal dynamics of an aquatic community. Therefore, what follows concentrates on the horizontal spatial structure of the marine environment.

Another important point is that the typical time of evolution of a given inhomogeneity should not be too short. The ocean is a multiscale system, and the adequacy of the assumption of its steadiness and/or homogeneity depends on the scale of the process of interest. The characteristic time of a plankton system is usually defined as the period it takes for the community to double in abundance. Roughly estimated, this varies from a few hours to a few days for phytoplankton species and from a few days to several weeks for zooplankters. Thus, a distinct spatial structure of a marine planktonic system can be expected to develop if induced by environmental inhomogeneities with a typical lifetime of not less than one month.

According to one definition, *plankton* is the collective name for marine organisms poorly adapted for active motion. Therefore, the first apparent cause of the formation of spatial structures in plankton systems is water movements. There is an extensive literature concerned with velocity fields of such motion in the world's ocean (see, for instance, Refs [210 – 212] and references therein). In a broader sense, this problem constitutes the principal issue in modern physical oceanography. The nature of velocity field heterogeneity depends on the scale of a given process. For example, on a small scale (from several centimeters to a few dozens of meters), this heterogeneity is mainly due to water turbulence and has the form of stochastic turbulent pulsations. On a large scale (hundreds of kilometers and more), the heterogeneity of velocity fields takes the form of oceanic currents and is induced by planetary-scale processes, e.g. such that ensue from interrelations between different climatic zones and the rotation of the Earth [213]. On intermediate scales (from several to tens of kilometers) the inhomogeneity of velocity fields is usually due to the interaction between different factors, one of the most important being the impact of the wind. Field heterogeneity of (horizontal) advective currents apparently leads to the formation of spatial structures in plankton communities [214 – 218]; some of them are reported in Ref. [12]. However, a detailed consideration of the data pertinent to this problem is beyond the scope of the present paper which is mostly centred on the patterns arising from biological interactions unrelated to ocean hydrodynamics.

The influence of seawater turbulence on the functioning of an aquatic community via its impact on the feeding and growth rates has been reported in a number of papers [219 – 221]. Also, inhomogeneous turbulent mixing of oceanic water (intermittence, turbulent patches, rips, etc.) is a widely observed phenomenon [222, 223]. It is natural to expect that it should also contribute to the formation of spatial and spatio-temporal patterns in a plankton community. This inference, however, is not so self-evident as it may seem. The thing is that the intensity of turbulent mixing in the ocean varies not only in space but also rapidly changes in time. Some theoretical findings indicate that an isolated turbulent patch tends to decay with time [224, 225], the estimated decay time usually being much smaller than characteristic times of aquatic communities. Thus, intermittent seawater turbulence appears to influence spatially homogeneous time-

averaged parameters of community dynamics [226] rather than the initiation of spatial structures by environmental factors.

Today, the point of primary interest is the possibility of formation of spatial structures unrelated to direct induction by water motion. There are a variety of factors affecting the dynamics of an aquatic community via effects on the growth, mortality, and feeding rates, etc. In what follows, the main attention will be given to temperature fields, the reason being that temperature is considered to be one of the most important parameters controlling the abundance of aquatic species [12, 227, 228]. Many authors have reported a strong correlation between sea surface temperature and chlorophyll concentration (see, for instance, Refs [79, 229, 230]). On the other hand, due to recent progress in remote sensing technology, the properties of spatial temperature fields in the ocean are known better than the properties of other fields [231].

The spatial inhomogeneity of temperature distribution in the ocean is a result of many underlying processes. As mentioned above, the characteristic time of different temperature field anomalies depends on the spatial scale of the process involved. Planetary-scale processes may have characteristic times of many tens or hundreds of years. Specifically, temperature differences between climatic zones are responsible for a steady horizontal temperature gradient averaging approximately $0.01\,^{\circ}\mathrm{C}\ \mathrm{km}^{-1}$ [232]. The value of the spatially averaged climatic gradient provides a natural scale for measuring the 'intensity' of various temperature anomalies.

The smallest spatial scale of the temperature field is determined by turbulence. Usually, it differs significantly in horizontal and vertical directions due to effects of gravity and stratification. Vertical spatial inhomogeneities are related to turbulent pulsation and do not to exceed the 'Ozmidov length' L_{oz} [160, 226] which normally falls into the range from tens of centimeters to several meters. Lateral turbulent exchange generally has a somewhat complicated nature and depends on the scale of the underlying phenomenon [160, 161, 233]. However, spatial temperature inhomogeneity induced by turbulent pulses can hardly produce any stable spatial structure in an aquatic community because the amplitude of temperature fluctuations is small (on the order of $0.1\,^{\circ}\mathrm{C}$) [233]. Also, the periods of fluctuations do not usually exceed a few minutes [233], being much smaller than temporal scales that characterize the functioning of aquatic communities.

Another mechanism for the formation of inhomogeneous temperature fields is vertical convection. Although, in certain cases, the processes underlying this phenomenon are not well understood [234], a widely accepted hypothesis suggests that free vertical convection results from hydrodynamic instability arising because the water density in the upper ocean layer is higher than in the subsurface one due to evaporation and cooling. The development of this instability can lead to the formation of a cell structure at the sea surface with alternating cold and warm patches, each underlain by a column of descending or ascending water respectively [235, 236]. The typical size of these patches in the ocean is estimated at 10 to 100 m and the characteristic time of their evolution from a few tens of minutes to several hours, with the temperature difference between cold and warm patches rarely exceeding $1\,^{\circ}\mathrm{C}$ [159]. It is worthwhile to note that vertical convection strongly affects the dynamics of pelagic communities, being responsible for seasonal disturbances of thermocline and upwelling of nutrient-rich warm water. However, free vertical convection can hardly be expected to contribute to the formation of a distinct long-living horizontal spatial structure in a pelagic community because of its relatively small spatial scale and non-stationary nature.

An example of a stable long-living spatial structure in a temperature field is provided by ocean fronts. The term ocean front is normally applied to an ocean region where the gradient of a certain parameter, e.g. temperature, salinity, and/or density, is much higher than its characteristic value for a given sector of the world's ocean [237]. With respect to temperature, such a typical value is given by the average climatic gradient. In practice, a temperature field in the ocean is usually considered to create a front when $|\nabla T| \geqslant 0.5-1.0\,^{\circ}\mathrm{C}\ \mathrm{km}^{-1}$. Special literature [232, 237] contains a great number of examples of ocean fronts differing in terms of structure, behaviour, and underlying physical mechanisms. A brief review of their properties that can be important in the context of this paper indicates that the temperature difference across the front varies from less than 1 to $5-6\,^{\circ}\mathrm{C}$. The width of the front (i.e. its characteristic size along the temperature gradient) usually lies between a few hundreds of meters and several kilometers while its length (extension along the front) varies from tens to several hundred kilometers. As regards the inner spatial structure, ocean fronts are usually either stepwise (sometimes, multistep), when the front separates regions with cold and warm water, or intermittent, when regions with cold and warm water alternate (also, cases of more complicated geometry may occur).

A remarkable property of ocean fronts is that they usually exist quite a long time, from a few months (seasonal fronts) to many years (e.g. fronts created by large-scale ocean currents), that is much longer than the characteristic time of a plankton system. Also, the temperature difference of a few °C across the front is often sufficient to markedly change the growth rate of phytoplankton species [12]. Another important point is that water on either side of the front usually comes from different sources and may thus significantly differ in nutrient levels, e.g. in the case of upwelling fronts. It appears that the combination of these two factors may be responsible for an 'imposed' spatial structure in the pelagic community [238, 239]. Indeed, some studies indicate that both the phytoplankton growth rate and the biomass of a pelagic community may be somewhat different on either side of the front [229, 239].

Ocean fronts give a typical but not the sole example of long-living inhomogeneities in an ocean temperature field. Another widely observed phenomenon leading to a relatively stable spatial structure are mesoscale (synoptic) eddies or 'rings' [240]. Eddies usually have a horizontal size from tens to 250–350 km and thickness from several hundred meters to slightly more than 1 km. They exist for a few weeks to several months. Mechanisms by which eddies are formed vary from one hydrographic region to another (see, for instance, Refs [241–244]). Eddies can be either 'warm' (when water temperature inside the ring is higher than outside) or 'cold', with the maximum temperature difference amounting to 10–12 °C. Besides the temperature, other factors (e.g. salinity and nutrient concentration) inside and outside a ring may be significantly different too.

An important point is that, regardless of their origin and peculiarities of hydrophysical structure, virtually all rings exhibit anomalous 'biological activity' [245], i.e. enhanced density of different plankton species and phytoplankton

growth rates. Moreover, the plankton community inside a ring can be spatially structured [246 – 248]. Some authors also report an increased abundance of certain fish species associated with eddies [249]. Another biologically important effect is due to the high mobility of such rings. While ocean fronts are usually localized in a certain region, synoptic rings can travel many hundreds of miles. In some cases, this may lead to a large-scale biological invasion when big masses of water containing a pelagic community are brought from the ring origin to another place occupied by a different community [250].

Also worthy of mention is a specific type of synoptic eddy known as rotating lens-like eddies (called meddies if they occur in the Northeastern Atlantic) [251 – 253]. Unlike an 'ordinary' synoptic ring with the volume of rotating water bordering the ocean surface, a lens as a whole is localized at depth. Typically, a lens leaves no observable traces at the ocean surface which makes it difficult to observe. This probably accounts for the scant information available on biological phenomena associated with rotating lenses. Nevertheless, because lenses exist like isolated water parcels with properties different from those of the surrounding water, they provide an good example of long-living inhomogeneities in ocean hydrophysical and hydrochemical fields. It is expected that further studies will bring more data on biological anomalies associated with this phenomenon [254].

It may be concluded that this brief examination of the properties of heterogeneous ocean fields (especially temperature fields) has demonstrated the presence of stable spatial structures (fronts and eddies) existing much longer than the typical time of plankton system dynamics. There is extensive evidence of the impact of these environmental patterns on the functioning of marine ecosystems. This provides a basis for the construction of models taking into account externally induced spatial structures in aquatic communities. An example of such a model will be considered in the next section.

5. Chaotic and regular plankton dynamics in spatially structured fish and plankton communities

5.1 Formulating the task

A brief revision of the main patterns in the marine environment (see Section 4) shows that spatio-temporal dynamics of aquatic communities is greatly affected by stable mesoscale structures. It should be noted that the temporal dynamics of a community may strongly depend on the spatial structure of its environment [255, 256]. In this section, we focus on the dynamics of plankton populations in a patchy environment. A minimal one-dimensional 'reaction – diffusion' model of plankton dynamics within a patch is considered on the assumption that some plankton habitats are rich in fish while others are not. We study the temporal behaviour of spatially averaged zooplankton and phytoplankton densities depending on such ecologically important parameters as fish predation rate on zooplankton and patch-to-patch distance. We show that diffusive interlinks between different habitats in a heterogeneous marine environment where some patches are inhabited by fish and others are not can give rise to plankton spatial patterns. We also demonstrate that spatially averaged plankton dynamics depending on the fish predation rate and the distance between fish-populated habitats can exhibit both chaotic and regular behaviour. Chaotic plankton dynamics occurs over a wide parameter range.

5.2. Model

We consider the basic four-component marine food chain model described by Eqns (3.3), (3.4). A simple explicit difference scheme is used for numerical integration of these equations. The one-dimensional space is divided into a grid of 64 finite-difference cells of unit length. The borderline between habitats divides the entire space into two patches. The time step is set equal to 10^{-2}. Repetition of integration at a smaller step showed that the numerical results did not change testifying to the accuracy of the chosen time step. The dynamics was investigated on the assumption of no-flux boundary conditions. The initial distributions of h and p in Eqns (3.3), (3.4) were taken to be uniform and the same for each habitat.

The diffusion terms in Eqns (3.3), (3.4) frequently describe spatial mixing of species due to active motions of individual organisms [96, 169]. In natural waters, however, it is turbulent diffusion that is supposed to dominate plankton mixing [92, 146]. Taking this into account, both phytoplankton and zooplankton may be regarded as a passive admixture transported by turbulent water flows. Therefore, in Eqns (3.3), (3.4), $d_p = d_h = d$. Using the relationship between the turbulent diffusion and the spatial scale of the phenomenon of interest [92, 160, 161], at the minimal phytoplankton growth rate $R_0 = 10^{-6}\ \mathrm{s}^{-1}$ [52] and characteristic length L/k (see Section 3) of plankton patches around 2 km, it can be shown that d is about 5×10^{-2}.

5.3 Two-patch ecosystem dynamics

Figure 13 shows system (3.3), (3.4) solution diagrams, i.e. the dependence of steady-state solutions on the fish predation rate. Evidently, phytoplankton-dominated stationary states are associated with a high predation rate f of fish feeding on zooplankton. A decrease of f results in one unstable and one more stable state thus making the system bistable. At a further decrease of f, both the phytoplankton-dominated stable steady-state and the unstable state disappear in a

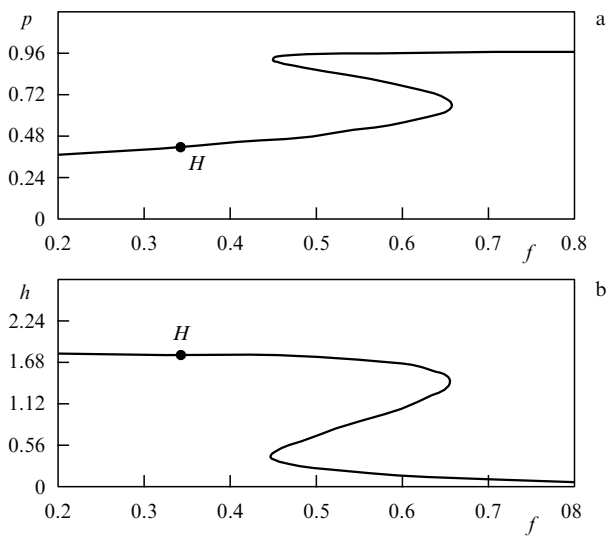

Figure 13. Model (3.3), (3.4) solution diagrams for the following set of parameters: $r = 5$, $a = b = 5$, $m = 0.6$, $n = 0.4$. The curves display steady-state solutions for different f. H shows the Hopf bifurcation.

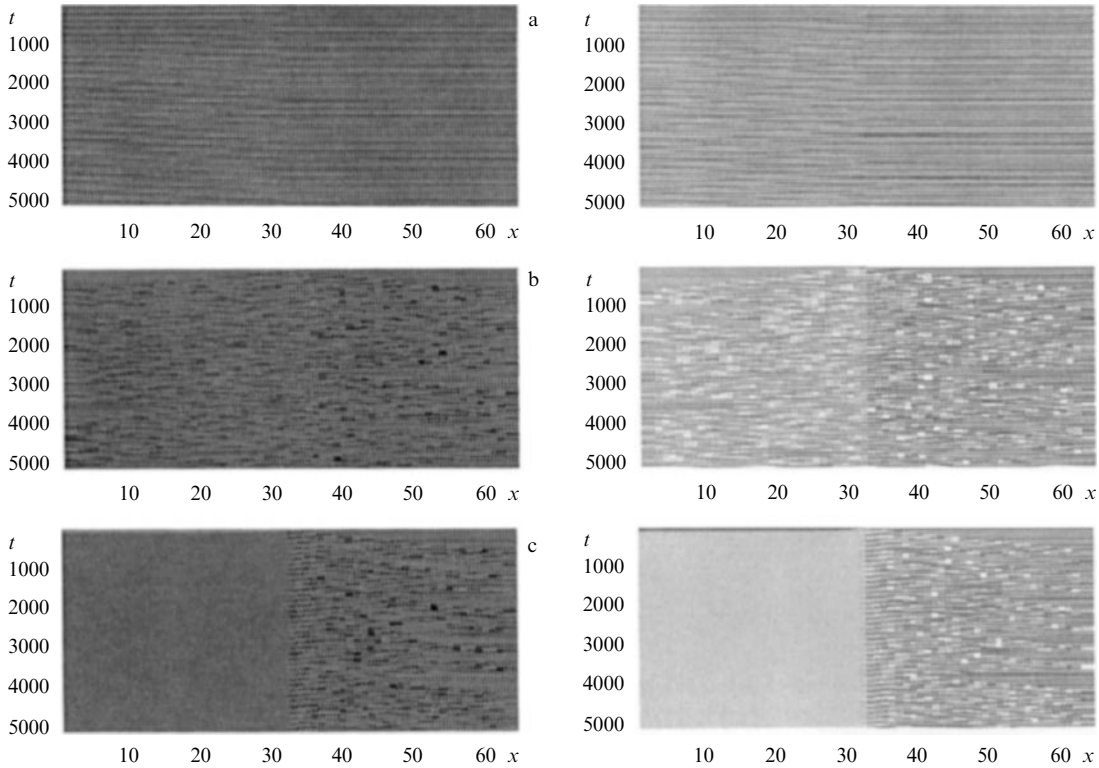

Figure 14. Spatio-temporal plankton patterns (left column: phytoplankton, right column: zooplankton) that emerged from the initially homogeneous distributions in a system of two habitats: for (a) $f = 0.05$, (b) $f = 0.18$, and (c) $f = 0.395$; x is the spatial coordinate, t is time.

saddle–node bifurcation. For even lower f, a Hopf bifurcation occurs at point H which causes destabilization of the zooplankton-dominated steady-state while creating a stable limit cycle. This means that, in the absence of fish ($f = 0$), the local kinetics of the system is oscillatory (for parameters corresponding to the solution diagram in Fig. 13). A deeper analysis of local properties of models similar to (3.3), (3.4) has been undertaken in Refs [44, 71, 147, 257].

Let us consider the simplest example of a spatially structured ecosystem consisting of only two patches. In both patches, the dynamics obey Eqns (3.3), (3.4), but for one of them $f = 0$, i.e. the fish density is negligibly small (for example, due to local changes in temperature or salinity). Figure 14 shows three sets of one-dimensional plankton spatial patterns which have emerged from the initially (at $t = 0$) homogeneous plankton distributions as a result of the diffusion interaction between a habitat populated by fish [at $x \leqslant 32$ with $f = 0.05$ (Fig. 14a), $f = 0.18$ (Fig. 14b), and $f = 0.395$ (Fig. 14c)] and another one ($x > 32$) where fish are absent ($f = 0$). It readily appears from the consideration of the dependence of the steady-state solution of system (3.3), (3.4) on the fish predation rate (see Fig. 13) that the values of $f = 0.05$ and $f = 0.18$ correspond to oscillatory plankton kinetics while $f = 0.395$ corresponds to the zooplankton-dominated steady state. It can be seen that, in the fish-populated habitat, an increase in the fish predation rate is followed by the transition from rather regular plankton patterns (see Fig. 14 at $f = 0.05$) to irregular ones (see Fig. 14 at $f = 0.18$) and thereafter to virtually unstructured plankton distributions (see Fig. 14 at $f = 0.395$). In the fish-free habitat, the transition is from regular (Fig. 14a) to irregular (Fig. 14b, c) patterns. Note that interlinks between the habitats are essential for perturbation of the initially homogeneous distributions; no pattern can form in their absence.

In order to demonstrate the dependence of plankton spatial patterns on the predation rate of zooplanktivorous fish in more detail, a pattern bifurcation diagram was constructed. Figure 15 shows plankton abundance as a function of coordinate x (horizontal axis) calculated at $t = 5000$ for different f (vertical axis), from 0 to 0.395. It can be seen that, for the fish-populated habitat, structures of large inner scale characteristic of smaller f values transform into small-scale irregular patterns as f increases. After the system passes the Hopf bifurcation, the transformation

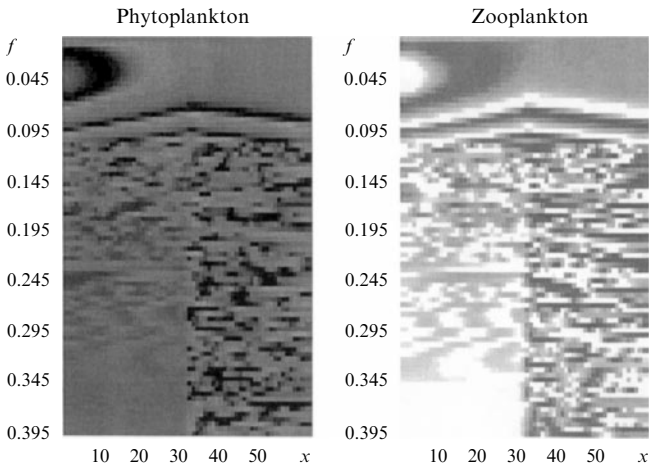

Figure 15. Phytoplankton and zooplankton pattern bifurcation diagram obtained after 500,000 iterations; x is the spatial coordinate, f is the fish predation rate on zooplankton.

continues to nearly homogeneous plankton distributions (see Fig. 13). In contrast, in the fish-free habitat, the Hopf bifurcation is not accompanied by substantial changes of the plankton structure (see Fig. 15). It also appears that phytoplankton density is lower in regions where zooplankton abounds and vice versa. Such an inverse relationship between phytoplankton and zooplankton was reported in many earlier studies as an apparent consequence of zooplankton grazing on phytoplankton [71].

Although the differences between the three main types of planktonic structures shown in Fig. 14 are well-apparent, it appears appropriate to characterize them in a more quantitative way, i.e. to ascribe a certain numerical index to each of the patterns. Also, it seems important to consider the transformation of one pattern to another in more detail in order to understand how the properties of the structures change for small variations of f. For this purpose, plankton spatio-temporal patterns (like those in Fig. 14) were converted to two-level structures for which densities below a threshold value were taken to be zero while those exceeding it were set equal to 1. The threshold value was chosen as the minimum peak of spatially averaged plankton density achieved in the course of pattern formation. Note the absence of differentiation between space and time for the identification of peculiar features characterizing spatio-temporal dynamics of the system.

To characterize the 'integral' properties of 'two-dimensional' spatio-temporal plankton patterns, we used the fractal dimension (D) of the two-level plankton structures described above and studied the dependence of D on the predation rate f of fish feeding on zooplankton. It should be noted that small changes in both the threshold and the range of t do not significantly influence the results of plankton pattern analysis; in this sense, these results should be regarded as rough ones.

Figure 16 demonstrates functions $D(f)$ obtained for zooplankton patterns in both fish-populated (Fig. 16a) and fish-free (Fig. 16b) habitats. (Because of the inverse relationship between phytoplankton and zooplankton density distributions, phytoplankton patterns are characterized by qualitatively similar functions.) The comparison of Figs 15 and 16 indicates that each $D(f)$ plateau corresponds to more regular plankton distributions. This tendency is more conspicuous at small f in the fish-populated habitat and at large f in the fish-free one. Functions $D(f)$ expose some new details of plankton patterns. Specifically, smooth changes of D inherent in the fish-populated habitat are accompanied by an abrupt change of the fractal dimension in the fish-free habitat (cf. Figs 16a and 16b). Therefore, plankton spatio-temporal dynamics in the fish-free habitat appears to be less stable with respect to changes in the fish predation rate than in the fish-populated habitat.

To study temporal plankton dynamics, both $|\mathbf{p}_i(t)|$ and $|\mathbf{h}_i(t)|$ were used, i.e. the vector lengths characterizing phytoplankton and zooplankton densities in each habitat:

$$\mathbf{p}_i(t) = \left(p_{i1}(t), p_{i2}(t), \ldots, p_{ik/2}(t)\right), \tag{5.1}$$

$$\mathbf{h}_i(t) = \left(h_{i1}(t), h_{i2}(t), \ldots, h_{ik/2}(t)\right), \tag{5.2}$$

as well as phytoplankton and zooplankton densities spatially averaged over each of these habitats:

$$\langle p\rangle_i(t) = \frac{1}{S_i}\int_{S_i} p(x,y,t)\,\mathrm{d}x\,\mathrm{d}y\,, \tag{5.3}$$

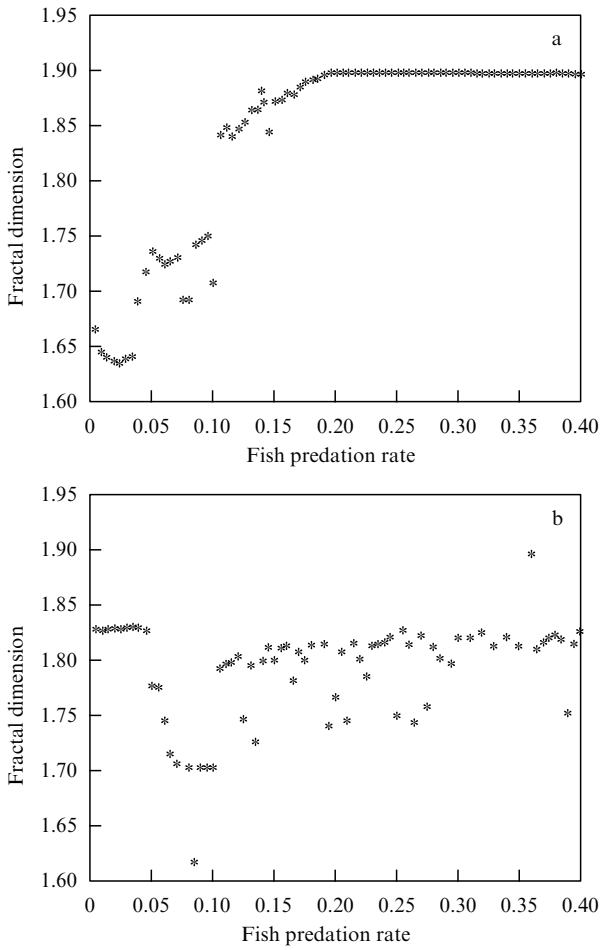

Figure 16. Dependence of the fractal dimension of zooplankton spatio-temporal patterns on the fish predation rate for fish-populated (a) and fish-free (b) habitats.

$$\langle h\rangle_i(t) = \frac{1}{S_i}\int_{S_i} h(x,y,t)\,\mathrm{d}x\,\mathrm{d}y\,, \tag{5.4}$$

where S_i is the area of the ith habitat, $i = 1$ corresponds to the fish-populated and $i = 2$ to the fish-free habitat, $S_1 = S_2 = k^2/2$ and $k = 64$. The two approaches yield qualitatively similar results.

Functions (5.1), (5.2) and (5.3), (5.4) turned out to strongly depend on the fish predation rate f. By way of example, Figs 17a and 17b demonstrate the dynamics of space-averaged zooplankton density $\langle h\rangle_i$ for fish-populated and fish-free habitats respectively. There are three main types of dynamics: regular oscillations (when f is small), irregular oscillations in both fish-populated and fish-free patches (when f increases), and virtually constant plankton density in the fish-populated patch and irregular oscillations in the fish-free habitat (when f grows further and becomes higher than the critical value characteristic of the Hopf bifurcation, see Fig 13). The same three types of dynamics occur for $|\mathbf{h}_i(t)|$.

The temporal behaviour of phytoplankton resembles that of zooplankton.

There is an obvious correspondence between the three types of averaged density temporal behaviour (see Fig. 17) and spatio-temporal patterns in Fig. 14. Regular and irregular patterns are responsible for regular and irregular oscillations of both $\langle p\rangle_i$ and $\langle h\rangle_i$ and $|\mathbf{p}_i(t)|$ and $|\mathbf{h}_i(t)|$

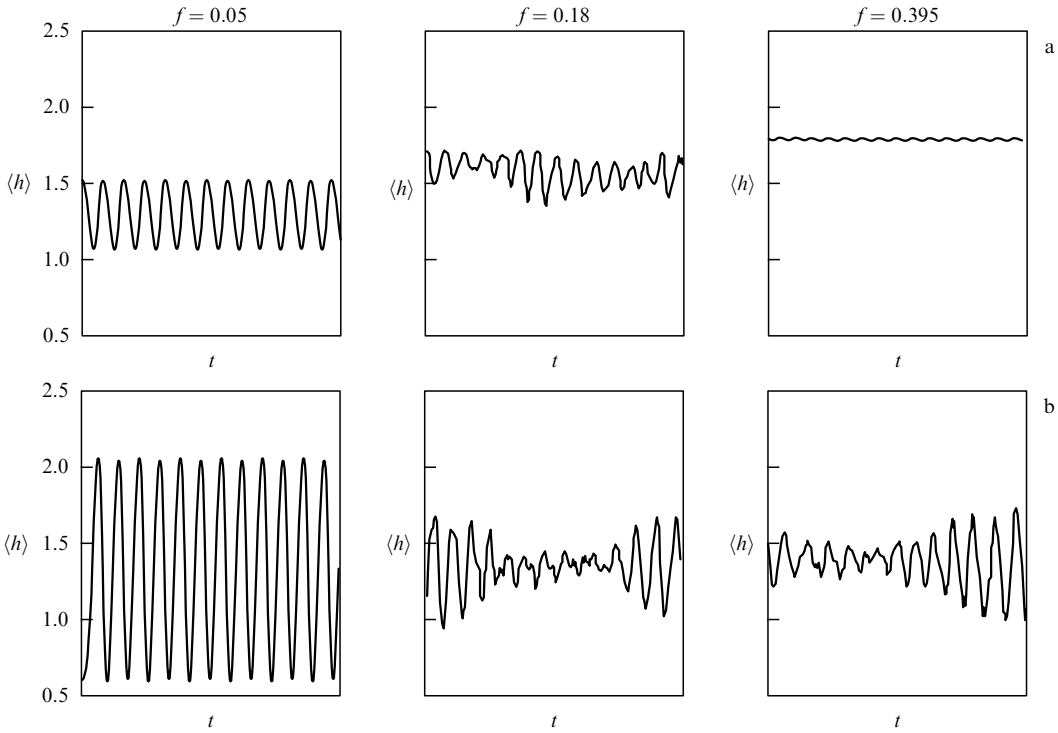

Figure 17. Three main types of oscillations of space-averaged zooplankton density depending on f: (a) at $x \leqslant 32$ (fish-populated habitat); (b) at $x > 32$ (fish-free habitat).

respectively whereas nearly homogeneous distributions lead to a practically constant plankton density.

It is noteworthy that irregular regimes, unlike regular ones, exhibit sensitivity to the initial conditions (Fig. 18); such dependence characterizes chaotic dynamics. Whether such chaotic behaviour is common for two-patch planktonic systems was investigated by constructing bifurcation diagrams for both fish-populated and fish-free habitats.

Figure 19 presents bifurcation diagrams for fish-populated (a) and fish-free (b) habitats. They show successive local maxima of time-dependent spatially averaged plankton densities for the corresponding fish predation rates on zooplankton over a range of f that covers all types of dynamics (see Fig. 17). Regular oscillations produce one or a small number of points whereas the successive maxima of irregular changes in plankton density are spread over rather a wide range of values. The diagrams were obtained after all transition processes were over, and the effect of the initial conditions became insignificant, allowing selected types of plankton dynamics to be fully manifested. Note the qualitatively different regions in the diagrams. At high fish predation rates, the fish-populated habitat displays regular plankton dynamics (Fig. 19a) while it is irregular in the fish-free patch (Fig. 19b; an example of such dynamics at $f = 0.395$ is shown in Fig. 17). For smaller f values, the regular dynamic patterns in the fish-populated patch are lost, and the maxima occur throughout the entire range of values excepting a very narrow gap in the vicinity of $f = 0.2$, where the dynamics becomes regular again (Fig. 19a). The example shown in Fig. 17 at $f = 0.18$ demonstrates irregular dynamics in the two patches. At $f < 0.1$, the plankton dynamics in both fish-populated and fish-free patches is regular (cf. Figs 19a and 19b; an example of such dynamics at $f = 0.05$ is given in Fig. 17). To provide a more quantitative insight into the nature of the temporal dynamics of averaged densities, we also computed the dominant Lyapunov exponent (λ). The results obtained for different predation rates of zooplankton-eating species in fish-populated (Fig. 19c) and fish-free (Fig. 19d) habitats are in good agreement with the bifurcation diagrams (Fig. 19a, b) and clearly demonstrate the chaotic nature of irregular plankton dynamics. Indeed, comparison of Figs 19a and 19c as well as Figs 19b and 19d shows that $\lambda > 0$ and chaos always occur at f values for which the regularity of plankton dynamics is broken. Our calculations indicate that, for irregular oscillations, at least the four first Lyapunov exponents are positive. This means that the irregular

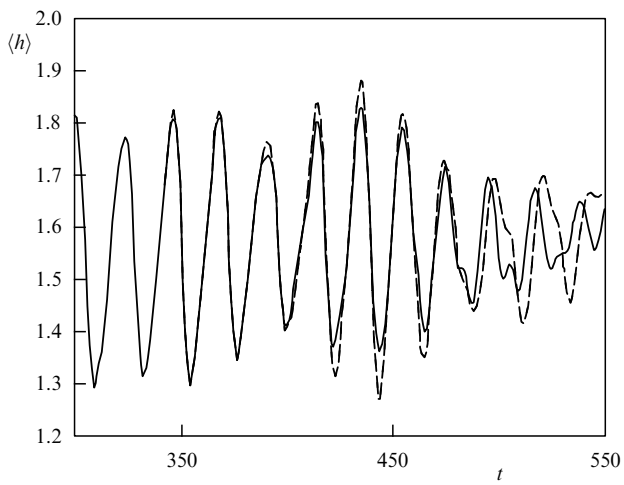

Figure 18. Sensitivity to initial conditions. Temporal oscillations $\langle h \rangle$ diverge for a minor change of the initial conditions. Trajectories of $\langle h \rangle$ are shown for two initial conditions differing by 0.001; $f = 0.18$.

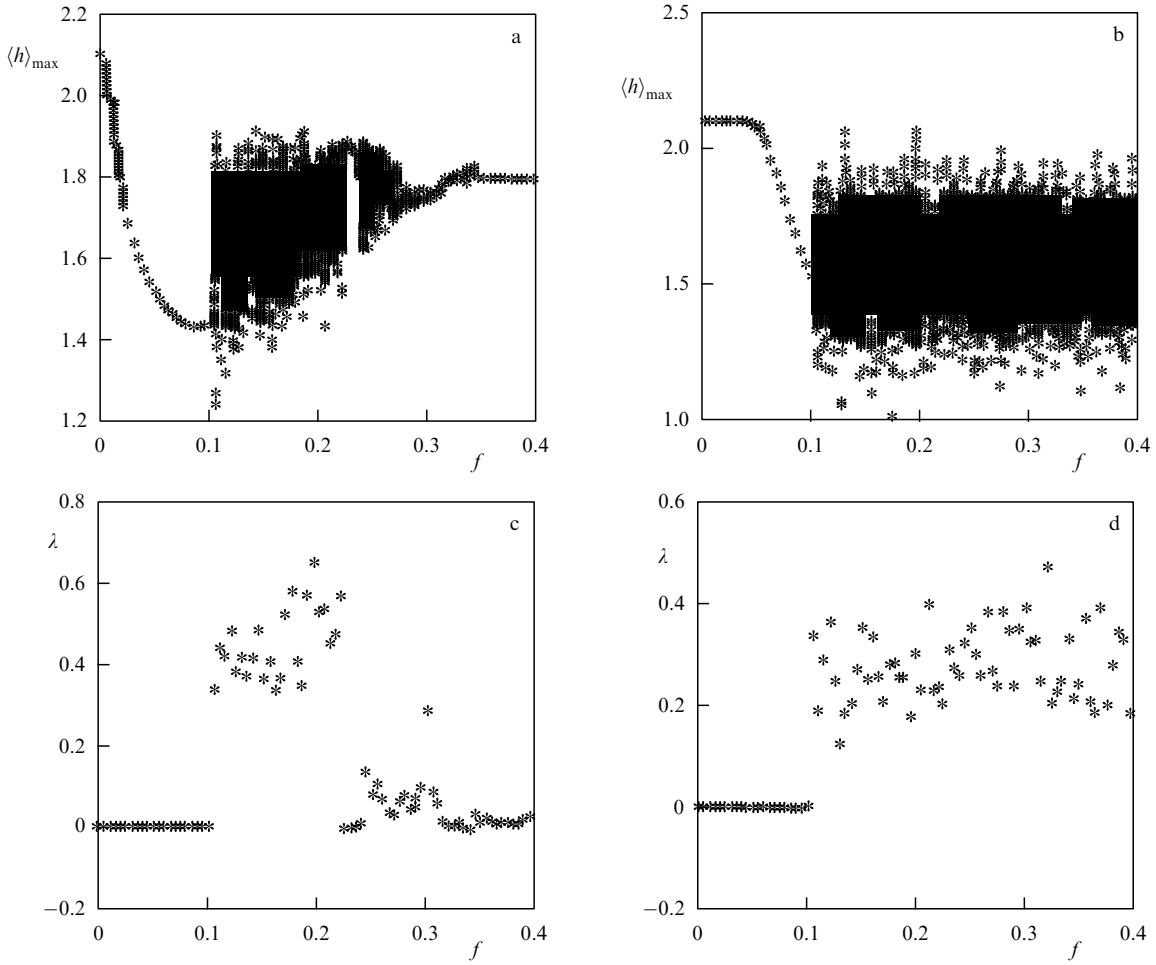

Figure 19. Bifurcation diagrams and dominant Lyapunov exponents at different fish predation rates f. (a) Bifurcation diagram for the fish-populated patch. (b) Bifurcation diagram for the fish-free patch. (c) Dominant Lyapunov exponent for the fish-populated patch. (d). Dominant Lyapunov exponent for the fish-free patch. All calculations were carried out in the time interval $2000 \leqslant t \leqslant 5000$.

plankton dynamics may be regarded as high-dimensional chaos.

It is worth noting that the dependence of plankton dynamics on the initial conditions is not reduced to the example shown in Fig. 18. Another type of such dependence is illustrated by Fig. 20. This figure shows two attractors obtained at slightly different initial zooplankton densities but with identical sets of model (3.3), (3.4) parameters. It can be seen that even minor changes of the initial conditions may lead to both regular oscillations (Fig. 20a) and chaotic variations (Fig. 20b) of plankton density. This suggests the existence of two attraction basins, each associated with one of the two attractors.

Interestingly, there is a large region of initial plankton density conditions in which the basin of attraction to the limit cycle is interlaid in a complicated manner with the chaotic attraction basin. Figure 21 shows the initial conditions (in a range of $|\mathbf{h}_1(0)| = |\mathbf{h}_2(0)|$ values from 0.3 to 2.7) leading either to a limit cycle (Fig. 20a) or to a chaotic attractor (Fig. 20b). The latter are shown as white sectors while the initial densities leading to regular oscillations are coloured black. It can be seen that, by increasing the resolution within a selected sector (e.g. $1.8 \leqslant |\mathbf{h}_1(0)| = |\mathbf{h}_2(0)| \leqslant 2.55$), additional details can be visualized giving evidence that the black zones (continuous at first sight) are actually broken into separate small parts. The higher the accuracy with which the borderline between the

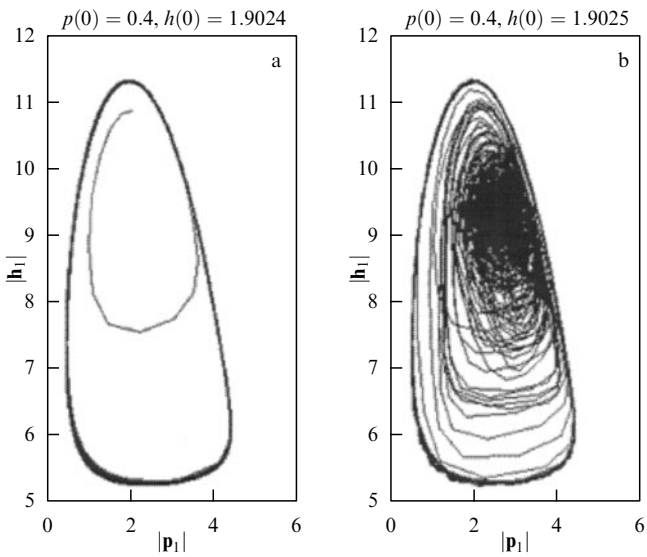

Figure 20. Sensitivity to initial conditions. The stable limit cycle (a) and chaotic attractor (b) obtained for somewhat different initial zooplankton densities; the difference is 0.0001; $f = 0.18$.

Figure 21. Fractal structure of attraction basins. The initial conditions leading to a chaotic attractor are shown as white sectors while the initial densities leading to regular oscillations are coloured black.

attraction basins is determined, the more jagged it looks (Fig. 21). The basins of attraction to regular and chaotic oscillations for these zooplankton density values are fractal, of Cantor set type. This accounts for the difficulty, if not impossibility, of prediction of which basin of attraction determines a given trajectory. To be correct, such a prediction must be based on exact information about the initial conditions. Even a weak noise renders the system unpredictable. There is, however, a continuous, non-fractal region of the initial conditions adjacent to the quantity $|\mathbf{h}_1(0)| = |\mathbf{h}_2(0)| = 2.7$. All trajectories originating in this region lead to a chaotic attractor (Fig. 21).

5.4 Three-patch ecosystem dynamics

Figure 22a presents an example of plankton spatial patterns emerging from an initially uniform distribution in a three-patch system consisting of two fish-populated habitats separated by a fish-free gap. The chosen parameters correspond either to the steady-state local kinetics [$f = 0.395$ in Fig. 22a(1)] or to the limit cycle local kinetics [$f = 0.18$ in Fig. 22a(2)]. The question is how the type of plankton dynamics depends on the width of the fish-free gap.

To answer this question, the dominant Lyapunov exponent for various gap widths (δ) was calculated. It appears that regular oscillations (similar to those in Fig. 17 at $f = 0.05$) are independent of δ. In Fig. 22b, λ is plotted versus δ for two other types of plankton dynamics (see Fig. 17). The function $\lambda(\delta)$ is explicitly nonmonotonic in the case of irregular plankton density oscillations in both the fish-populated patches and the fish-free gap separating them (Fig. 22b at $f = 0.18$). Note that there is a close correlation between the gap width-dependent variations of the dominant Lyapunov exponent characterizing plankton dynamics in the fish-populated patches (solid line) and the fish-free gap (dashed line). Such a correlation is absent for a practically constant plankton density in the fish-populated patches whereas the fish-free gap undergoes irregular oscillations of this parameter (Fig. 22b at $f = 0.395$). It is easy to see that in the fish-populated patches λ is virtually constant and equal to zero while in the fish-free gap it monotonically decreases to zero as the gap width becomes smaller approaching 14 (the bottom of Fig. 22b). To conclude, these results indicate that in a natural heterogeneous environment plankton dynamics in a given habitat may depend not only on local habitat-specific parameters (such as the fish predation rate on zooplankton) but also on patch-to-patch distances.

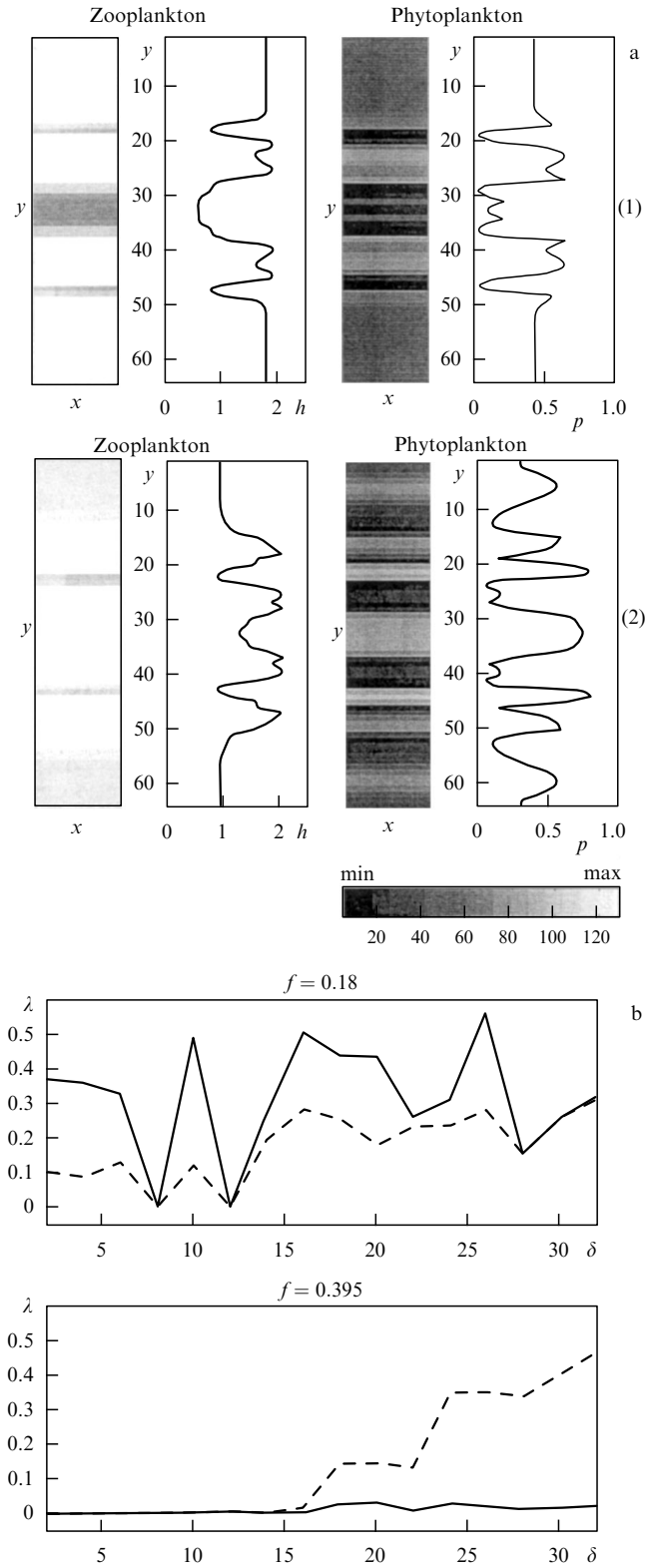

Figure 22. (a) Quasi-2D spatial patterns of zooplankton and phytoplankton emerging in a three-patch system of the initially uniform plankton distribution and corresponding plankton density profiles for $x \leqslant 16$ and $48 \leqslant x \leqslant 64$, (1) $f = 0.395$ or (2) $f = 0.18$ while for $16 < x < 48$ $f = 0$. (b) Dependence of dominant Lyapunov exponents in fish-populated (solid line) and fish-free (dashed line) habitats on the distance between fish-populated habitats.

6. Brief summary

This work updates readers on the processes underlying the dynamics of spatially inhomogeneous aquatic communities. It is well-known that the non-uniform spatial distribution of different species cannot be invariably reduced to the heterogeneity of the marine environment because it is governed by physical as well as biological factors. The paper considers different mechanisms of the formation of intrinsic biological patterns, i.e. patterns not directly related to any aspect of ocean hydrodynamics. It is shown that the formation of spatial structures in the plankton distribution resembling natural ones (i.e. irregular structures with a finite lifetime) may come about as an immediate result of the interplay between turbulent mixing and phytoplankton-zooplankton interactions. The formation of a plankton pattern is characterized by an intrinsic spatial scale the size of which (estimated to be on the order of 1 km) is consistent with the results of field observations.

The minimal model used in this work as sufficient to describe the formation of the irregular spatially non-uniform plankton distribution is a two-species predator – prey (phytoplankton – zooplankton) system with the parameters independent of coordinates and free from constraints on the diffusion coefficients which make up the system of components. The system dynamics corresponding to the spatial pattern formation may be regarded as spatio-temporal chaos. The appearance of irregular spatial distributions (in the case of an unusual development scenario) may be preceded by the formation of distinct spiral patterns.

Another mechanism of formation of irregular spatial patterns in a plankton community may be related to the impact of a planktivorous fish school. The interaction between a mobile fish school and a plankton system, although modifying the properties of its spatial structure, leaves the major features of the system dynamics unaltered, i.e. generation of spiral waves and chaos. The fish school motion has been shown to possess fractal properties.

A review of field observation data has demonstrated that in many cases the dynamics of an aquatic community is subject to effects of relatively stable mesoscale inhomogeneities inherent in ecologically significant factors, such as water temperature, salinity, nutrient concentration, etc. The characteristic size of these inhomogeneities determines one more (external) scale of the system. The paper analyses plankton pattern formation and the associated spatio-temporal community dynamics in an inhomogeneous environment. A minimal reaction – diffusion model of the nutrient – plankton – fish food chain is used to evaluate the role of diffusive interrelations between fish-populated and fish-free habitats in a patchy environment in plankton pattern formation. It is shown that such interactions may give rise to spatio-temporal plankton patterns of fractal dimension depending on the fish predation rate. The spatially averaged plankton dynamics turns out to be a function of both fish predation rates and distances between fish-populated habitats; it exhibits chaotic as well as regular behaviour.

The results reported in this paper (see also Ref. [265]) demonstrate the critical role of chaotic regimes in the spatio-temporal organization of aquatic ecosystems. Indeed, there is a growing body of evidence that systems with chaotic dynamics have a higher adaptive potential under changing environmental conditions than systems with a stable equilibrium point [57, 258 – 261]. At the level of the organism, the existence of chaos and related irregularities may indicate well-being [262, 263]. Certain authors go so far as to argue that aging is related to the loss of plasticity and variability afforded by chaos in basic physiological systems [263]. Hence, the great interest of the problem of the interrelations between chaotic and regular dynamics.

This paper illustrates new challenges created by an improved understanding of the importance of non-linear interactions in the dynamics of aquatic communities. Conceptual few-species reaction – diffusion models appear to be an adequate tool for discovering and elucidating fundamental mechanisms of spatio-temporal pattern formation in coupled plankton-fish dynamics.

The authors are grateful to Valeriĭ Prostokishin for assistance in numerical experiments. Thanks are also due to Andreĭ Kostyanoĭ who read the manuscript and made useful remarks.

The work was partially supported by INTAS (grant 96-2033), DFG (grant 436 RUS 113/447), RFBR (grant 98-04-04065), and NATO (grant OUTR.LG971248).

References

1. Haken H *Synergetics. An Introduction* (Springer Series in Synergetics, Vol. 1) (Berlin: Springer-Verlag, 1977)
2. Nicolis G, Prigogine I *Self-organization in Nonequilibrium Systems* (New York: Wiley, 1977)
3. Weidlich W, Haag G *Concepts and Models of a Quantitative Sociology. The Dynamics of Interacting Populations* (Springer Series in Synergetics, Vol. 14) (Berlin: Springer-Verlag, 1983)
4. Turing A M *Philos. Trans. R. Soc. London Ser. B* **237** 37 (1952)
5. Medvinsky A B et al., in *Self-organization of Complex Structures. From Individual to Collective Dynamics* (Ed. F Schweitzer) (Amsterdam: Gordon and Breach Sci. Publ., 1997) p. 269
6. De Kepper P et al. *Physica D* **49** 161 (1991)
7. Shemyakin F M, Mikhalev P F *Fiziko-Khimicheskie Periodicheskie Protsessy* (Physico-Chemical Periodic Processes) (Moscow – Leningrad: Izd. AN SSSR, 1938)
8. Romanovskiĭ Yu M, Stepanova N V, Chernavskiĭ D S *Matematicheskaya Biofizika* (Mathematical Biophysics) (Moscow: Nauka, 1984)
9. Sommer U *Planktologie* (Berlin: Springer, 1994)
10. Sommer U *Algen, Quallen, Wasserfloh. Die Welt des Planktons* (Berlin: Springer, 1996)
11. Baretta-Bekker J G, Duursma E K, Kuipers B R (Eds) *Encyclopedia of Marine Sciences* 2nd ed. (New York: Springer, 1998)
12. Raymont J E G *Plankton and Productivity in the Oceans* (Oxford: Pergamon Press, 1980 – 1983)
13. Hallegraeff G M *Plankton. A Microscopic World* (Leiden: E.J. Brill, 1988)
14. Hensen V *Ergebnisse in dem Atlantischen Ocean von Mitte Juli bis Anfang November 1889 ausgeführten Plankton-Expedition der Humboldt-Stiftung* (Leipzig: Kiel, 1892)
15. Porep R, in *Kieler Beiträge zür Geschichte der Medizin und Pharmazic* Vol. 9 (Eds R Herrlinger, F Kudlien, G E Dann) (Neumünster: Karl Wachholtz, 1970)
16. Bain R C (Jr.) *J. Sanitary Engineering Division* (October) 867 (1968)
17. Ritschard R L *Water Air Soil Poll.* **64** 289 (1992)
18. Malin G *Nature* **387** 857 (1997)
19. Charlson R J et al. *Nature* **326** 655 (1987)
20. Williamson P, Gribbin J *New Sci.* (16 March) 48 (1991)
21. Lotka A J *Elements of Physical Biology* (Baltimore: Williams & Wilkins Co., 1925)
22. Volterra V *J. Cons. Perm. Int. l'Explor. Mer.* **3** 3 (1926)
23. Cushing D H *Marine Ecology and Fisheries* (Cambridge: Cambridge Univ. Press, 1975)
24. Gulland J A (Ed.) *Fish Population Dynamics* (London: Wiley, 1977)
25. Steele J H (Ed.) *Fisheries Mathematics: The Proc. of a Conf., Aberdeen, 1975* (London: Academic Press, 1977)
26. Fleming R H *J. Cons. Perm. Int. l'Explor. Mer.* **14** 210 (1939)

27. Ivlev V S *Usp. Sovremennoĭ Biol.* **XIX** 98 (1945)
28. Riley G A *J. Mar. Res.* **6** 54 (1946)
29. Odum H T *Limnol. Oceanogr.* **1** 102 (1956)
30. Droop M R *Bot. Mar.* **XXVI** 99 (1983)
31. Behrenfeld M J, Falkowski P G *Limnol. Oceanogr.* **42** 1479 (1997)
32. Riley G A, in *The Sea* Vol. 2 (Ed. M N Hill) (London: Wiley, 1963) p. 436
33. Segel L A, Jackson J L *J. Theor. Biol.* **37** 545 (1972)
34. Dubois D *Ecol. Model.* **1** 67 (1975)
35. Levin S A, Segel L A *Nature* **259** 659 (1976)
36. Mimura M, Murray J D *J. Theor. Biol.* **75** 249 (1978)
37. Mayzaud P, Poulet S A *Limnol. Oceanogr.* **23** 1144 (1978)
38. Holling C S *Can. Entomol.* **91** 385 (1959)
39. Michaelis L, Menten M *Biochem. Z.* **49** 333 (1913)
40. Monod J, Jacob F *Cold Spring Harb. Symp.* **26** 389 (1961)
41. Steele J H, Henderson E W *Am. Nat.* **117** 676 (1981)
42. Steele J H, Henderson E W *J. Plankton Res.* **14** 157 (1992)
43. Steele J H, Henderson E W *J. Plankton Res.* **14** 1397 (1992)
44. Scheffer M *OIKOS* **62** 271 (1991)
45. Scheffer M *Ecology of Shallow Lakes* (Population and Community Biology Series, Vol. 22) (London: Chapman & Hall, 1997)
46. Malchow H *Proc. R. Soc. London Ser. B* **251** 103 (1993)
47. Truscott J E, Brindley J *Bull. Math. Biol.* **56** 981 (1994)
48. Truscott J E, Brindley J *Philos. Trans. R. Soc. London Ser. A* **347** 703 (1994)
49. Beltrami E *Estuaries* **12** 13 (1989)
50. Beltrami E *Environ. Model. Assess.* **1** 19 (1996)
51. De Angelis D L *Dynamics of Nutrient Cycling and Food Webs* (Population and Community Biology Series, Vol. 9) (London: Chapman & Hall, 1992)
52. Jörgensen S E *Fundamentals of Ecological Modelling* 2nd ed. (Amsterdam: Elsevier, 1994)
53. Yodzis P, in *Frontiers in Mathematical Biology* (Lecture Notes in Biomathematics, Vol. 100, Ed. S A Levin) (Berlin: Springer-Verlag, 1994)
54. May R *Science* **186** 645 (1974)
55. Scheffer M *J. Plankton Res.* **13** 1291 (1991)
56. Godfray C, Hassell M *Science* **275** 323 (1997)
57. Huisman J, Weissing F J *Nature* **402** 407 (1999)
58. Pascual M *Proc. R. Soc. London Ser. B* **251** 1 (1993)
59. Petrovskii S V, Malchow H *Math. Comput. Model.* **29** 49 (1999)
60. Petrovskii S V, Malchow H *Theor. Popul. Biol.* **59** 157 (2001)
61. Evans G T, Parslow S *Biol. Oceanogr.* **3** 327 (1985)
62. Truscott J E *J. Plankton Res.* **17** 2207 (1995)
63. Popova E E et al. *J. Plankton Res.* **19** 1495 (1997)
64. Ascioti F A et al. *J. Plankton Res.* **15** 603 (1993)
65. Kuznetsov Yu A, Muratori S, Rinaldi S *Int. J. Bifurcat. Chaos* **2** 117 (1992)
66. Rinaldi S, Muratori S *Ecol. Model.* **69** 79 (1993)
67. Steffen E, Malchow H, in *Self-organization of Complex Structures. From Individual to Collective Dynamics* (Ed. F Schweitzer) (Amsterdam: Gordon and Breach Sci. Publ., 1997) p. 331
68. Steffen E, Malchow H *Senckenbergiana Maritima* **27** 137 (1996)
69. Steffen E, Malchow H, Medvinsky A B *Environ. Model. Assess.* **2** 43 (1997)
70. Scheffer M et al. *OIKOS* **80** 519 (1997)
71. Fasham M J R *Oceanogr. Mar. Biol. Ann. Rev.* **16** 43 (1978)
72. Steele J H (Ed.) *Spatial Pattern in Plankton Communities* (NATO Conf. Ser. IV, Marine Sciences, Vol. 3) (New York: Plenum Press, 1978)
73. Mackas D L, Boyd C M *Science* **204** 62 (1979)
74. Greene C H et al. *Limnol. Oceanogr.* **37** 650 (1992)
75. Abbott M, in *Patch Dynamics* (Lecture Notes in Biomathematics, Vol. 96, Eds S A Levin, T M Powell, J H Steele) (Berlin: Springer-Verlag, 1993) p. 37
76. Novikov I Ya, Stechkin S B *Usp. Mat. Nauk* **53** (6) 53 (1998) [*Russ. Math. Surv.* **53** 1159 (1998)]
77. Dremin I M, Ivanov O V, Nechitaĭlo V A *Usp. Fiz. Nauk* **171** 465 (2001) [*Phys. Usp.* **44** 447 (2001)]
78. Platt T *Deep-Sea Res.* **19** 183 (1972)
79. Denmann K L *Deep-Sea Res.* **23** 539 (1976)
80. Stommel H *J. Mar. Res.* **8** 24 (1948)
81. Leibovich S, in *Patch Dynamics* (Lecture Notes in Biomathematics, Vol. 96, Eds S A Levin, T M Powell, J H Steele) (Berlin: Springer-Verlag, 1993) p. 110
82. Yoder J A et al. *Nature* **371** 689 (1994)
83. Franks P J S *Limnol. Oceanogr.* **42** 1297 (1997)
84. Abraham E R *Nature* **391** 577 (1998)
85. Platt J R *Science* **133** 1766 (1961)
86. Winet H, Jahn T *Biorheology* **9** 87 (1972)
87. Pedley T J, Kessler J O *Ann. Rev. Fluid Mech.* **24** 313 (1992)
88. Timm U, Okubo A *Bull. Math. Biol.* **56** 187 (1994)
89. Witten T A (Jr.), Sander L M *Phys. Rev. Lett.* **47** 1400 (1981)
90. Matsushita M, Fujikawa H *Physica A* **168** 498 (1990)
91. Ben-Jacob E et al. *Physica A* **87** 378 (1992)
92. Okubo A *Diffusion and Ecological Problems. Mathematical Models* (Biomathematics, Vol. 10) (Berlin: Springer-Verlag, 1980)
93. Holmes E E et al. *Ecology* **75** 17 (1994)
94. Malchow H *Ecol. Model.* **75/76** 123 (1994)
95. Kierstead H, Slobodkin L B *J. Mar. Res.* **XII** 141 (1953)
96. Skellam J G *Biometrika* **38** 196 (1951)
97. Luther R *Z. Electrochemie* **12** 596 (1906)
98. Fisher R A *Ann. Eugenics* **7** 355 (1937)
99. Kolmogorov A, Petrovskii I, Piskunov N *Bull. Univ. Moscow, Ser. Intern. Sect. A* **1** 1 (1937)
100. Allee W C *Animal Aggregations: A Study in General Sociology* (Chicago: The Univ. of Chicago Press, 1931)
101. Allee W C et al. *Principles of Animal Ecology* (Philadelphia: Saunders Co., 1949)
102. Schlögl F *Z. Phys.* **253** 147 (1972)
103. Nitzan A, Ortoleva P, Ross J *Faraday Symp. Chem. Soc.* **9** 241 (1974)
104. Ebeling W, Schimansky-Geier L, in *Proc. 6th Intern. Conf. on Thermodynamics* (Merseburg, 1980) p. 95
105. Malchow H, Schimansky-Geier L *Noise and Diffusion in Bistable Nonequilibrium Systems* (Teubner-Texte zur Physik, Bd. 5) (Leipzig: Teubner, 1985)
106. Lewis M A, Kareiva P *Theor. Popul. Biol.* **43** 141 (1993)
107. Petrovskiĭ S V *Inzh. Fiz. Zh.* **66** 398 (1994) [*J. Eng. Phys. Thermophys.* **66** 346 (1994)]
108. Ludwig D, Jones D D, Holling C S *J. Anim. Ecol.* **47** 315 (1978)
109. Wissel C *Theoretische Ökologie* (Berlin: Springer, 1989)
110. Field R J, Burger M (Eds) *Oscillations and Traveling Waves in Chemical Systems* (New York: Wiley, 1985)
111. Wyatt T *Mar. Biol.* **22** 137 (1973)
112. Boerlijst M C, Lamers M E, Hogeweg P *Proc. R. Soc. London Ser. B* **253** 15 (1993)
113. Adler J *Science* **153** 708 (1966)
114. Adler J, Templeton B *J. Gen. Microbiol.* **46** (Pt. 2) 175 (1967)
115. Gerisch G, in *Current Topics in Developmental Biology* Vol. 3 (Eds A A Moscona, A Monroy) (New York: Academic, 1968) p. 157
116. Gerisch G *Naturwissenschaften* **58** 430 (1971)
117. Keller E F, Segel L A *J. Theor. Biol.* **26** 399 (1970)
118. Keller E F, Segel L A *J. Theor. Biol.* **30** 225 (1971)
119. Keller E F, Segel L A *J. Theor. Biol.* **30** 235 (1971)
120. Segel L A, Stoeckly B *J. Theor. Biol.* **37** 561 (1972)
121. Segel L A *SIAM J. Appl. Math.* **32** 653 (1977)
122. Newell P C, in *Fungal Differentiation. A Contemporary Synthesis* (Mycology Series, Vol. 4, Ed. J E Smith) (New York: M. Dekker, 1983) p. 43
123. Alt W, Hoffmann G (Eds) *Biological Motion* (Lecture Notes in Biomathematics, Vol. 89) (Berlin: Springer-Verlag, 1990)
124. Ivanitskiĭ G R, Medvinskiĭ A B, Tsyganov M A *Usp. Fiz. Nauk* **161** (4) 13 (1991) [*Sov. Phys. Usp.* **34** 289 (1991)]
125. Ivanitskiĭ G R, Medvinskiĭ A B, Tsyganov M A *Usp. Fiz. Nauk* **164** 1041 (1994) [*Phys. Usp.* **37** 961 (1994)]
126. Medvinsky A B et al. *FEMS Microbiol. Lett.* **84** 279 (1991)
127. Medvinsky A B et al. *FEMS Microbiol. Lett.* **112** 287 (1993)
128. Medvinsky A B et al. *Physica D* **64** 267 (1993)
129. Medvinsky A B et al. *Physica D* **79** 299 (1994)
130. Medvinskiĭ A B et al. *Dokl. Ross. Akad. Nauk* **338** 690 (1994)
131. Siegert F, Weijer C J *Physica D* **49** 224 (1991)
132. Steinbock G, Hashimoto H, Müller S C *Physica D* **49** 233 (1991)
133. Reshetilov A N et al. *FEMS Microbiol. Lett.* **94** 59 (1992)

134. Vasiev B N, Hogeweg P, Panfilov A V *Phys. Rev. Lett.* **73** 3173 (1994)
135. Höfer T, Sherratt J A, Maini P K *Physica D* **85** 425 (1995)
136. Sherratt J A, Lewis M A, Fowler A C *Proc. Natl. Acad. Sci. USA* **92** 2524 (1995)
137. Sherratt J A, Eagan B T, Lewis M A *Philos. Trans. R. Soc. London Ser. B* **352** 21 (1997)
138. Merkin J H et al. *Phys. Rev. Lett.* **76** 546 (1996)
139. Davidson F A *Int. J. Bifurcat. Chaos* **8** 1303 (1998)
140. Rovinsky A B, Menzinger M *Phys. Rev. Lett.* **69** 1193 (1992)
141. Malchow H *J. Marine Syst.* **7** 193 (1996)
142. Malchow H *Z. Phys. Chem.* **204** 35 (1998)
143. Daly K L, Smith W O (Jr.) *Ann. Rev. Ecol. Syst.* **24** 555 (1993)
144. O'Brien J J, Wroblewski J S *J. Theor. Biol.* **38** 197 (1973)
145. Wroblewski J S, O'Brien J J, Platt T *Mémoires Soc. R. Sci. Liège* **VII** 43 (1975)
146. Wroblewski J S, O'Brien J J *Mar. Biol.* **35** 161 (1976)
147. Malchow H, Shigesada N *Nonlinear Proc. Geophys.* **1** 3 (1994)
148. Wyatt T *Thalassia Jugoslavica* **7** 435 (1971)
149. Nakata K, Ishikawa R *Jpn. J. Ecol.* **25** 201 (1975)
150. Powell T M et al. *Science* **189** 1088 (1975)
151. Weber L H, El-Sayed S Z, Hampton I *Deep-Sea Res.* **33** 1327 (1986)
152. Murray J D *Mathematical Biology* (Berlin: Springer-Verlag, 1989)
153. Levin S A, Powell T M, Steele J H (Eds) *Patch Dynamics* (Lecture Notes in Biomathematics, Vol. 96) (Berlin: Springer-Verlag, 1993)
154. Dunbar S R *SIAM J. Appl. Math.* **46** 1057 (1986)
155. Petrovsky S V, Vinogradov M E, Morozov A Yu *Okeanologiya* **38** 881 (1998) [*Oceanology* **38** 796 (1998)]
156. Petrovskii S V, Malchow H *Nonlinear Anal.: Real World Appl.* **1** 37 (2000)
157. Kopell N, Howard L N *Stud. Appl. Math.* **52** 291 (1973)
158. Nayfeh A H, Balachandran B *Applied Nonlinear Dynamics* (New York: Wiley, 1995)
159. Fedorov K N, Ginzburg A I *Pripoverkhnostnyĭ Sloĭ Okeana* (The Subsurface Layer in the Ocean) (Leningrad: Gidrometeoizdat, 1988)
160. Ozmidov R V *Gorizontal'naya Turbulentnost' i Turbulentnyĭ Obmen v Okeane* (Horizontal Turbulence and Turbulent Exchange in the Ocean) (Moscow: Nauka, 1968)
161. Okubo A *Deep-Sea Res.* **18** 789 (1971)
162. Petrovskii S V *J. Marine Syst.* **21** 179 (1999)
163. Ozmidov R V *Okeanologiya* **38** 7 (1998) [*Oceanology* **38** 3 (1998)]
164. Holland J H *Adaptation in Natural and Artificial Systems* (Ann Arbor: Univ. of Michigan Press, 1975)
165. Scheffer M et al. *Ecol. Model.* **80** 161 (1995)
166. Savill N J, Hogeweg P *J. Theor. Biol.* **184** 229 (1997)
167. Radakov D V *Staĭnost' Ryb Kak Ekologicheskoe Yavlenie* (Schooling in the Ecology of Fish) (Moscow: Nauka, 1972) [Translated into English (New York: J. Wiley, 1973)]
168. Blake R W *Fish Locomotion* (Cambridge: Cambridge Univ. Press, 1983)
169. Okubo A *Adv. Biophys.* **22** 1 (1986)
170. Semovskiĭ S V *Mat. Modelirovanie* **1** (6) 49 (1989)
171. Grünbaum D, Okubo A, in *Frontiers in Mathematical Biology* (Lecture Notes in Biomathematics, Vol. 100, Ed. S A Levin) (Berlin: Springer-Verlag, 1994) p. 296
172. Huth A, Wissel C *Ecol. Model.* **75/76** 135 (1994)
173. Reuter H, Breckling B *Ecol. Model.* **75/76** 147 (1994)
174. Gueron S, Levin S A, Rubenstein D I *J. Theor. Biol.* **182** 85 (1996)
175. Niwa H-S *J. Theor. Biol.* **181** 47 (1996)
176. Romey W L *Ecol. Model.* **92** 65 (1996)
177. Flierl G et al. *J. Theor. Biol.* **196** 397 (1999)
178. Stöcker S *Math. Biosci.* **156** 167 (1999)
179. Goodwin R M, in *Socialism, Capitalism and Economic Growth* (Ed. C H Feinstein) (London: Cambridge Univ. Press, 1967) p. 54
180. Lorenz H-W *Nonlinear Dynamical Economics and Chaotic Motion* 2nd ed. (Berlin: Springer-Verlag, 1993)
181. Ruth M, Hannon B *Modeling Dynamic Economic Systems* (New York: Springer, 1997)
182. Malchow H et al. *Nonlinear Anal.: Real World Appl.* **1** 53 (2000)
183. Medvinsky A B et al. *Nonlinear Dynam. Psychol. Life Sci.* **4** 135 (2000)
184. Tikhonov D A et al. *Chaos Soliton. Fract.* **12** 277 (2000)
185. Tikhonova I A et al. *Biofiz.* **45** 352 (2000) [*Biophys.* **45** 343 (2000)]
186. Bocharov L N *Sistemnyĭ Analiz v Kratkosrochnom Rybopromyslovom Prognozirovanii* (Systemic Analysis in Short-Term Fishery Forecasts) (Leningrad: Nauka, 1990)
187. Ebenhöh W *Model. Ident. Control* **1** 69 (1980)
188. Fernö A et al. *Sarsia* **83** 149 (1998)
189. Misund O A et al. *Sarsia* **83** 117 (1998)
190. Murray J D *Lectures on Nonlinear-Differential-Equation Models in Biology* (Oxford: Clarendon, 1977)
191. Winfree A T *The Geometry of Biological Time* (Biomathematics, Vol. 8) (New York: Springer-Verlag, 1980)
192. Winfree A T *When Time Breaks Down* (Princeton, N.J.: Princeton Univ. Press, 1987)
193. Krinskiĭ V I, Medvinskiĭ A B, Panfilov A V *Evolyutsiya Avtovolnovykh Vikhreĭ. Volny v Serdtse* (Evolution of Autowave Vortices. Waves in the Heart) (Moscow: Znanie, 1986)
194. Grusa K-U *Mathematical Analysis of Nonlinear Dynamic Processes* (Harlow: Longman Scientific & Technical, 1988)
195. Biktashev V N et al. *Phys. Rev. Lett.* **81** 2815 (1998)
196. Mandelbrot B B *Fractals: Form, Chance, and Dimension* (San Francisco: W.H. Freeman, 1977)
197. Mandelbrot B B *The Fractal Geometry of Nature* (San Francisco: W.H. Freeman, 1982)
198. Feder J *Fractals* (New York: Plenum Press, 1988)
199. Schroeder M R *Fractals, Chaos, Power Laws* (New York: W.H. Freeman, 1991)
200. Peitgen H-O, Jürgens H, Saupe D *Chaos and Fractals: New Frontiers of Science* (New York: Springer-Verlag, 1992)
201. Bacry E, Muzy J F, Arneodo A *J. Stat. Phys.* **70** 635 (1993)
202. Arneodo A et al. *Physica D* **96** 291 (1996)
203. Muzy J F, Bacry E, Arneodo A *Phys. Rev. E* **47** 875 (1993)
204. Arneodo A, Bacry E, Muzy J F *Physica A* **213** 232 (1995)
205. Meyer Y *Ondelettes et Opérateurs* (Paris: Hermann, 1989) [Translated into English: *Wavelets and Operators* (Cambridge: Cambridge Univ. Press, 1992)]
206. David G *Wavelets and Singular Integrals on Curves and Surfaces* (Berlin: Springer-Verlag, 1991)
207. Kahane J P, Lemarié-Rieusset P G *Fourier Series and Wavelets* (London: Gordon & Breach, 1995)
208. Hubbard B B *The World According to Wavelets. The Story of a Mathematical Technique in the Making* (Wellesley, Mass.: A K Peters, 1996)
209. Chhabra A B et al. *Phys. Rev. A* **40** 5284 (1989)
210. Phillips O M *The Dynamics of the Upper Ocean* 2nd ed. (Cambridge: Cambridge Univ. Press, 1977)
211. Pond S, Pickard G L *Introductory Dynamic Oceanography* (Oxford: Pergamon Press, 1978)
212. Pedlosky J *Geophysical Fluid Dynamics* 2nd ed. (New York: Springer-Verlag, 1987)
213. Pedlosky J *Ocean Circulation Theory* (Berlin: Springer, 1996)
214. Vozjinskaya V B *Oceanology* **4** 876 (1964)
215. Abbot M R, Zion P M *Cont. Shelf Res.* **4** 661 (1985)
216. Walsh J J et al. *Prog. Oceanogr.* **23** 245 (1989)
217. Capella J E et al. *Deep-Sea Res.* **39** 1201 (1992)
218. Sur H I et al. *J. Marine Syst.* **7** 293 (1996)
219. MacKenzie B R et al. *Limnol. Oceanogr.* **39** 1790 (1994)
220. Jenkinson I R, Biddanda B A *J. Plankt. Res.* **17** 2251 (1995)
221. Marrase C, Saiz E, Redondo J M (Eds) *Lectures on Plankton and Turbulence* (Scientia Marina, Vol. 61, Suppl. 1) (Barcelona: Intern. Centre for Coastal Resources Res., 1997)
222. Nihoul J C J (Ed.) *Marine Turbulence* (Elsevier Oceanography Series, Vol. 28) (Amsterdam: Elsevier, 1980)
223. Monin A S, Ozmidov R V *Okeanskaya Turbulentnost'* (Ocean Turbulence) (Leningrad: Gidrometeoizdat, 1981) [Translated into English: *Turbulence in the Ocean* (Dordrecht: Reidel, 1985)]
224. Barenblatt G I, Galerkina N L, Luneva M V *Inzh. Fiz. Zh.* **53** 733 (1987) [*J. Eng. Phys. Thermophys.* **53** 733 (1987)]
225. Barenblatt G I *Scaling, Self-similarity, and Intermediate Asymptotics* (Cambridge: Cambridge Univ. Press, 1996)
226. Ozmidov R V *Okeanologiya* **6** 393 (1966)
227. Laurs R M, Fidler P C, Montgomery D R *Deep-Sea Res.* **31** 1085 (1984)
228. Hofmann E E et al. *Deep-Sea Res.* **39** 1177 (1992)

229. Hood R R et al. *J. Geophys. Res.* **95** 18081 (1990)
230. Barnard A H, Stegmann P M, Yoder J A *Cont. Shelf Res.* **17** 1181 (1997)
231. Njoku E G et al. *J. Geophys. Res.* **90** 11573 (1985)
232. Rodionov V B, Kostyanoĭ A G *Okeanicheskie Fronty Moreĭ Severo-Evropeĭskogo Basseĭna* (Ocean Fronts in the North-European Basin) (Moscow: GEOS, 1998)
233. Monin A S, Kamenkovich V M, Kort V G *Izmenchivost' Mirovogo Okeana* (Variability of the World's Ocean) (Leningrad: Gidrometeoizdat, 1974) [Translated into English: *Variability of the Ocean* (New York: Wiley, 1977)]
234. Monin A S, Krasitskiĭ V P *Yavleniya na Poverkhnosti Okeana* (Surface Phenomena in the Ocean) (Leningrad: Gidrometeoizdat, 1985)
235. Foster T D, in *Processus de Formation des Eaux Oceaniques Profondes, en Particulier en Mediterranee Occidentale, Paris, 1972* (Colloques Intern. Du Centre National de la Recherche Scientifique, N 215) (Paris: CNRS, 1974) p. 237
236. Joseph D D *Stability of Fluid Motions* (Springer Tracts in Natural Philosophy, Vol. 27–28) (Berlin: Springer-Verlag, 1976)
237. Fedorov K N *Fizicheskaya Priroda i Struktura Okeanicheskikh Frontov* (Nature and Structure of Ocean Fronts) (Leningrad: Gidrometeoizdat, 1983) [Translated into English: *The Physical Nature and Structure of Oceanic Fronts* (Berlin: Springer-Verlag, 1986)]
238. Fiedler P C, Bernard H J *Cont. Shelf Res.* **7** 871 (1987)
239. Mackas D L, Washburn L, Smith S L *J. Geophys. Res.* **96** 14781 (1991)
240. Kamenkovich V M, Koshlyakov M N, Monin A S *Sinopticheskie Vikhri v Okeane* 2nd ed. (Synoptic Eddies in the Ocean) (Leningrad: Gidrometeoizdat, 1987) [Translated into English (Dordrecht: D. Reidel, 1986)]
241. Sverdrup H U *J. Mar. Res.* **1** 115 (1938)
242. The Ring Group *Science* **212** 1091 (1981)
243. The Coastal Transition Zone Group *EOS* **69** 669 (1988)
244. Barth J A *J. Geophys. Res.* **94** 10844 (1989)
245. Angel M V, Fasham M J R, in *Eddies in Marine Science* (Ed. A R Robinson) (Berlin: Springer-Verlag, 1983) p. 492
246. Haury L R et al. *J. Geophys. Res.* **91** 12937 (1986)
247. Hayward T L, Mantyla A W *J. Mar. Res.* **48** 825 (1990)
248. Bucklin A *J. Geophys. Res.* **96** 14799 (1991)
249. Bowman M J et al., in *Coastal Oceanography* (NATO Conf. Series, Ser. IV: Marine Sciences, Vol. 11, Eds H G Gade, A Edwards, H Svendsen) (New York: Plenum Press, 1983) p. 279
250. Wiebe P H et al. *Deep-Sea Res.* **23** 695 (1976)
251. Armi L, Zenk W *J. Phys. Oceanogr.* **14** 1560 (1984)
252. Armi L et al. *Nature* **333** 649 (1988)
253. Kostianoy A G, Belkin I M, in *Mesoscale/Synoptic Coherent Structures in Geophysical Turbulence* (Elsevier Oceanography Series, Vol. 50, Eds J C J Nihoul, B M Jamart) (Amsterdam: Elsevier, 1989) p. 821
254. Cooper L H N, in *Oceanography: Invited Lectures Presented at the Intern. Oceanographic Congress, New York, 1959* (Publ. AAAS, Vol. 67, Ed. M Sears) (Washington: AAAS, 1961) p. 599
255. Nisbet R M et al., in *Patch Dynamics* (Lecture Notes in Biomathematics, Vol. 96, Eds S A Levin, T M Powell, J H Steele) (Berlin: Springer-Verlag, 1993)
256. Ranta E, Kaitala V, Lundberg P *Science* **278** 1621 (1997)
257. Scheffer M *Hydrobiol. Bull.* **23** 73 (1989)
258. Wilson D S *Ecology* **73** 1984 (1992)
259. Allen J C, Scheffer W M, Rosko D *Nature* **364** 229 (1993)
260. Hastings A *Ecology* **74** 1362 (1993)
261. Pahl-Wostl C *Theor. Popul. Biol.* **43** 159 (1993)
262. Garfinkel A et al. *Science* **257** 1230 (1992)
263. West B J, Deering B *The Lure of Modern Science: Fractal Thinking* (Studies of Nonlinear Phenomena in Life Sciences, Vol. 3) (Singapore: World Scientific, 1995)
264. Marks-Tarlow T *Nonlinear Dynam. Psychol. Life Sci.* **3** 311 (1999)
265. Lipsitz L, Goldberger A *J. Am. Med. Assoc.* **267** 1806 (1992)
266. Medvinsky A B et al. *J. Bioscience* **26** 77 (2001)
267. Medvinsky A B et al. *J. Bioscience* **26** 109 (2001)
268. Astaf'eva N M *Usp. Fiz. Nauk* **166** 1145 (1996) [*Phys. Usp.* **39** 1085 (1996)]